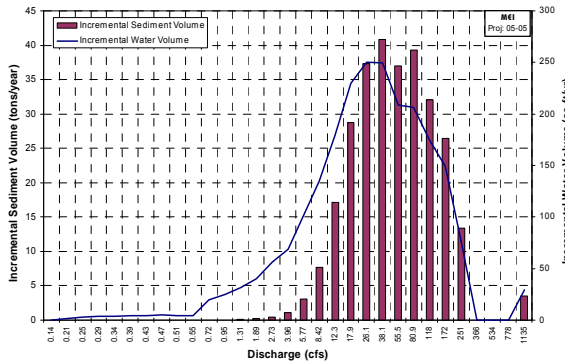
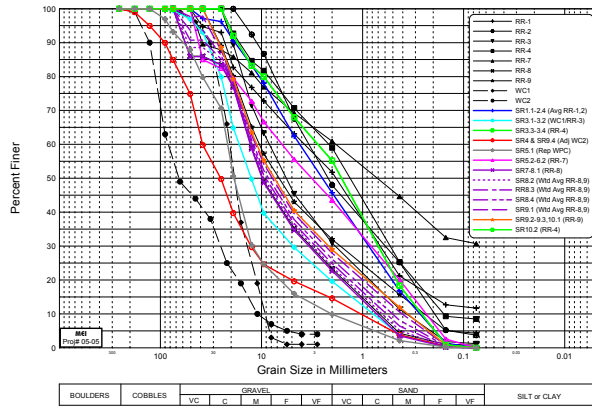


# TECHNICAL MEMORANDUM

## Sediment Transport

### Root River Sediment-transport Planning Study Contract No. W30003P01



Submitted to: **Milwaukee Metropolitan Sewerage District**  
260 West Seeboth Street  
Milwaukee, Wisconsin 53204



Submitted by: **Musser Engineering, Inc.**



September 7, 2007

# Table of Contents

	<u>Page</u>
1. INTRODUCTION.....	1
2. BACKGROUND INFORMATION .....	1
2.1. Subreach-averaged Hydraulic Results.....	1
2.2. Bed-material Sediment Data .....	2
3. INCIPIENT MOTION ANALYSIS.....	3
4. SEDIMENT-TRANSPORT CAPACITY .....	5
4.1. Selection of Sediment-Transport Formula.....	5
4.2. Sediment-transport Capacity Rating Curves .....	7
4.3. Annual Sediment-transport Volumes.....	9
4.4. Effective Discharge .....	9
5. SEDIMENT-TRANSPORT ANALYSIS—EXISTING CONDITIONS.....	10
6. SEDIMENT-TRANSPORT ANALYSIS—FUTURE CONDITIONS .....	12
7. EVALUATION OF LATERAL EROSION POTENTIAL.....	13
8. SUMMARY AND CONCLUSIONS.....	14
9. REFERENCES.....	15

## List of Figures

Figure 1.1.	Map of the North Branch Root River watershed showing the locations of the primary tributaries. Also shown are the locations of the sediment samples. ....	18
Figure 2.1.	Subreach-averaged main channel hydraulic depth profiles for flows ranging from the 50-percent mean daily exceedence flow to the 100-year peak event ...	20
Figure 2.2.	Subreach-averaged main channel velocity profiles for flows ranging from the 50-percent mean daily exceedence flow to the 100-year peak event. ....	21
Figure 2.3.	Subreach-averaged main channel topwidth profiles for flows ranging from the 50-percent mean daily exceedence flow to the 100-year peak event. ....	22
Figure 2.4.	Gradation curves for the bulk sediment samples and pebble counts collected on the North Branch Root River. Also shown are the representative subreach gradations used in the sediment-transport analysis.....	23

Figure 2.5. Gradation curves for the bulk sediment samples and pebble counts collected on the primary tributaries to the North Branch Root River. Also shown are the representative gradations used in the sediment-transport analysis ..... 23

Figure 3.1. Results from the incipient motion analysis and the representative median grain size, by subreach. (A dimensionless grain shear value of 1.0 indicates incipient-motion conditions, and a value of 1.5 indicates measurable transport). ..... 25

Figure 4.1a. Bed-material sediment-rating curves for the upstream supply and Subreaches 1.1 through 2.4. .... 26

Figure 4.1b. Bed material sediment rating curves for the upstream supply and Subreaches 3.3 through 7. .... 26

Figure 4.1c. Bed-material sediment-rating curves for the upstream supply and Subreaches 8.1 through 10.2. .... 27

Figure 4.2. Bed-material sediment rating curves for the primary tributaries to the North Branch Root River. .... 27

Figure 4.3. Existing conditions flow-duration curves at various locations along the North Branch Root River (see Technical Memorandum: Hydrology). .... 28

Figure 4.4. Existing conditions flow duration curves for the primary tributaries to the North Branch Root River (see Technical Memorandum: Hydrology). .... 28

Figure 4.5. Average annual sediment transport capacity volumes (by size class) for the subreaches in the North Branch Root River and in the primary tributaries. Also shown is the median grain size of the bed material..... 29

Figure 4.6. Example histogram of incremental bed-material load by discharge class for Subreach 6.2. Also shown is the incremental water volume within each discharge class..... 30

Figure 4.7. Results from the effective discharge analysis ..... 30

Figure 4.8. Histogram of incremental bed-material load by discharge class for Subreach 2.4. Also shown is the incremental water volume within each discharge class.. 31

Figure 5.1. Comparison of annual bed material transport capacity and supply for each subreach..... 32

Figure 5.2. Computed volume of aggradation or degradation, by size fraction, in each of the subreaches from the sediment-continuity analysis. Also shown is the corresponding average depth of aggradation and degradation..... 33

Figure 5.3. Comparative thalweg profiles for the North Branch Root River between 1966 and 2006 ..... 34

Figure 6.1. Future (2020) conditions flow-duration curves at various locations along the North Branch Root River (see Technical Memorandum: Hydrology). ..... 36

Figure 6.2. Future (2020) conditions flow duration curves for the primary tributaries to the North Branch Root River (see Technical Memorandum: Hydrology). ..... 36

Figure 6.3. Annual bed-material transport capacity volumes under existing and future (2020) hydrologic conditions for the subreaches in the North Branch Root River and the primary tributaries. .... 37

Figure 6.4. Computed annual volume of aggradation or degradation under existing and future (2020) hydrologic conditions for the subreaches in the North Branch Root River and the primary tributaries. Also shown is the corresponding change in bed elevation. .... 38

**List of Tables**

Table 2.1. Subreaches used in the sediment-continuity analysis..... 19

Table 2.2. Summary of representative subreach gradations..... 24

Table 5.1. Summary of computed aggradation/degradation depths and observed trends of aggradation and degradation, by subreach. .... 35

# Sediment-transport Technical Memorandum

## Root River Sediment-transport Planning Study

---

September 7, 2007

### 1. INTRODUCTION

The portion of the Root River that is the main subject of this investigation is the North Branch located in Milwaukee County. The reach extends about 17 miles upstream from the confluence with the Root River Canal to the Milwaukee-Waukeesha County Line (South 124<sup>th</sup> Street) (**Figure 1.1**). The primary purpose of this investigation was to provide the Milwaukee Metropolitan Sewerage District (MMSD) with an evaluation of the existing vertical and horizontal stability of the stream channels within the District's jurisdiction, and a tool to assess the impacts of future structural work within the watercourses for flood-management purposes or other purposes deemed necessary by the District. As part of this evaluation, a sediment-transport analysis of the mainstem North Branch Root River was carried out to evaluate tendencies for erosion and sedimentation under existing conditions, and to determine the potential effects of future development within the watershed on channel stability. The sediment transport analysis was carried out using hydrologic (see Technical Memorandum: Hydrology) and hydraulic information (see Technical Memorandum: Hydraulics), as well as information collected during the field reconnaissance to characterize the bed material (see Technical Memorandum: Geomorphology). In addition to the sediment transport analysis, a qualitative assessment of the potential for lateral erosion of the channel was also carried out.

### 2. BACKGROUND INFORMATION

Information that was necessary to conduct the sediment-transport analysis included estimates of the hydrologic and hydraulic conditions that were developed as part of this investigation and bed material data that was collected during the field reconnaissance.

#### 2.1. Subreach-averaged Hydraulic Results

Output from the HEC-RAS hydraulic model was used to generate subreach-averaged hydraulic characteristics for the ten geomorphic subreaches (see Technical Memorandum: Hydraulics). For the sediment-transport analysis, the project reach was subdivided into 28 subreaches to reflect the locations of vertical controls and the highly variable bed material characteristics (discussed in the following section). The subreach delineations for the sediment-transport analysis are presented in **Table 2.1** and Figure 1.1.

Subreach-averaged hydraulic characteristics (i.e., flow depth, topwidth, velocity, etc.) were developed from the HEC-RAS hydraulic model. The data indicate that the average main channel hydraulic depth at the 2-year event ranges from about 2.1 feet in Subreach 1.1 to about 7.5 feet in Subreach 10.2, with a general trend of increasing depth with increasing drainage area in the upstream portion of the reach, and no consistent trend in the downstream portion of the reach (**Figure 2.1**). Main channel velocities are highest in Subreach 1.1 due to the steep channel gradient, and in the subreaches with relatively narrow channel widths (Subreaches 8.3 through 9.1) (**Figure 2.2**). Average main channel topwidths increase significantly in the

downstream direction from Subreach 1.1 to Subreach 3.3 due to the increase in contributing drainage area. At the 2-year peak discharge, for example, the average topwidth in Subreach 1.1 is only about 18 feet, increasing to about 86 feet in Subreach 3.3 (**Figure 2.3**). Top widths are quite narrow in Subreach 4 (about 36 feet at the modeled flow peak flows) due to observed large woody debris-induced bank accretion (see Technical Memorandum: Geomorphology). Similar to the velocity profiles, there is no significant trend in the average topwidths through the remainder of the reach, although Subreaches 10.1 and 10.2 (the most downstream subreaches) are somewhat narrower, possibly the result of historic channel degradation.

## 2.2. Bed-material Sediment Data

Seven bulk samples (RR1-RR4, RR7-RR9) were collected along the North Branch Root River to characterize the bed material and the range of sizes that are transported by the flows. Additionally, two pebble counts (Wolman, 1954) were used to characterize the gradations of the coarser surface sediments that are delivered to the North Branch Root River by the steeper tributaries. Six bulk samples were collected on the primary tributaries that deliver significant amounts of sediment to the North Branch Root River, including samples at the mouths of Hale Creek, 104<sup>th</sup> Street Ditch, Tess Corners Creek, East Branch Root River, and two samples on Whitnall Park Creek. Two pebble counts were also conducted in Whitnall Park Creek where the surface bed material was composed primarily of gravels. The sample locations are shown on Figure 1.1.

Representative bed material gradations were developed for the 28 subreaches using the gradations of the samples and pebble counts (**Figures 2.4 and 2.5**), and supplementary field observations and photographs (**Table 2.2**). As discussed in later sections of this report, the sediment-transport formulae used in this analysis were developed for sand and gravel size fractions, and do not represent the transport of silts or clays that do not normally contribute a significant portion of the bed material. Therefore, the representative subreach gradations shown in Figures 2.4 and 2.5 were adjusted to remove the silt/clay portion.

The representative gradation for Subreaches 1.1 through 2.4 was based on the average gradation of Samples RR-1 (**Figure A.1**) and RR-2 (**Figure A.2**), since the bed material is generally composed of fine gravel in this reach and these samples have similar gradations. Subreaches 3.1 and 3.2 are coarser due to the sediment load delivered from 104<sup>th</sup> Street Ditch. The representative gradation for these subreaches was based on an average of the surface (armor layer) gradation represented by Pebble Count WC1 (**Figure A.3**) and the subsurface gradation from Sample RR-3 (**Figure A.4**) that characterize the bed material in the overall bed sediment reservoir. Sample RR-4 (**Figure A.5**) is located in Subreach 3.3 and was used as the representative gradation for Subreaches 3.3 and 3.4. In Subreach 4, the bed material is generally coarser than in the upstream subreaches due to erosion of non-cohesive glacial till deposits in the banks. Pebble Count WC2 (**Figure A.6**) was conducted to characterize this material on a representative coarse-grained riffle in the subreach, but does not represent the finer bed material up- and downstream from the riffles. The representative gradation for Subreach 4, therefore, was developed by adding sand to the tail of the gradation curve for Pebble Count WC2 and smoothing the remainder of the curve. The representative gradation from Whitnall Park Creek was used in Subreach 5.1 since the sediment load from this tributary is deposited in the bed of the North Branch Root River for some distance downstream from the confluence (**Figure A.7**). In Subreaches 5.2 through 6.2, the bed material significantly fines due to the presence of numerous large woody debris blockages. Sample RR-7 (**Figure A.8**) characterizes the material that is stored upstream from these blockages and its gradation was used for these subreaches. Sample RR-8 (**Figure A.9**) characterizes the relatively coarse

material in Subreaches 7 and 8.1, while Sample RR-9 (**Figure A.10**) was used for Subreaches 9.2 and 9.3. The bed material in between Samples RR-8 and RR-9 is generally composed of sandy gravel (**Figure A.11**). Because Sample RR-9 is slightly finer than Sample RR-8, the representative gradations in Subreaches 8.2 through 9.1 were based on a distance-weighted average of these two samples. The bed material in Subreach 9.4 is derived from the very coarse right bank terrace upstream from West Ryan Road and the observed sediment sizes (**Figure A.12**) are similar to the riffles in Subreach 4; thus, the representative gradation from Subreach 4 was adopted for this subreach. Downstream from Subreach 9.4, the bed material rapidly fines to sandy gravel that is characterized by Sample RR-9, which was used as the representative gradation for Subreach 10.1. In the downstream subreach (Subreach 10.2), the bed material is gravelly sand with a gradation similar to Sample RR-4.

Representative gradations for the primary tributaries were also developed to estimate the tributary sediment loading to the North Branch Root River. The representative tributary gradations were based on the furthest downstream sample (i.e., the sample nearest to the mouth), and included samples Hale-1 (**Figure A.13**), 104-1 (**Figure A.14**), WPC-1 (**Figure A.15**), and EB-1 (**Figure A.16**). For Whitnall Park Creek, the upper end of Sample WPC-1 was adjusted to include the same coarse bed material indicated in Pebble Count WPC2.

Based on the samples and their gradations (Figures 2.4 and 2.5), it is apparent that the bed material size varies significantly along the project reach of the North Branch Root River due to injection of local sources of sediment from both channel erosion and the tributaries. Unlike most alluvial streams, there is no downstream fining trend in the bed material.

### 3. INCIPIENT MOTION ANALYSIS

An incipient-motion analysis (i.e., an evaluation of flows required to move the bed material) was performed by evaluating the effective shear stress on the channel bed in relation to the amount of shear stress that is required to move the surface particles in each of the subreaches. The shear stress required for bed mobilization was estimated from the Shields (1936) relation, given by:

$$\tau_c = \tau_{*c} (\gamma_s - \gamma) D_{50} \quad (3.1)$$

where  $\tau_c$  = critical shear stress for particle motion,  
 $\tau_{*c}$  = dimensionless critical shear stress (often referred to as the Shields parameter),  
 $\gamma_s$  = unit weight of sediment (~165 lb/ft<sup>3</sup>),  
 $\gamma$  = unit weight of water (62.4 lb/ft<sup>3</sup>), and  
 $D_{50}$  = median particle size of the bed material.

In gravel-bed streams, when the critical shear stress for the median particle size is exceeded, the bed is mobilized and all sizes up to about 5 times the median size can be transported by the flow (Parker et al., 1982; Andrews, 1984).

Reported values for the Shields parameter range from 0.03 (Neill, 1968; Andrews, 1984) to 0.06 (Shields, 1936). A value of 0.047 is commonly used in engineering practice, based on the point at which the Meyer-Peter, Müller (MPM) bed-load equation indicates no transport (MPM, 1948). More recent evaluations of the MPM data and other data (Parker et al., 1982; Andrews, 1984) indicates that true incipient motion occurs at a value of about 0.03 in gravel- and cobble-bed

streams. Neill (1968) concluded that a dimensionless shear value of 0.03 corresponds to true incipient motion of the bed-material matrix while 0.047 corresponds to a low, but measurable transport rate. A value of 0.03 was used in this analysis.

In performing an incipient-motion analysis, the bed shear stress due to grain resistance ( $\tau'$ ) is used rather than the total shear stress, because it is a better descriptor of the near-bed hydraulic conditions that are responsible for sediment movement. The grain shear stress is computed from the following relation:

$$\tau' = \gamma Y' S \quad (3.2)$$

where  $Y'$  = the portion of the total hydraulic stress associated with grain resistance (Einstein, 1950), and  
 $S$  = the energy slope at the cross section.

The value of  $Y'$  is computed by iteratively solving the semi-logarithmic velocity profile equation:

$$\frac{V}{V_*'} = 6.25 + 5.75 \log \frac{Y'}{K_s} \quad (3.3)$$

where  $V$  = mean velocity at the cross section,  
 $K_s$  = characteristic roughness of the bed, and  
 $V_*'$  = shear velocity due to grain resistance given by:

$$V_*' = \sqrt{g Y' S} \quad (3.4)$$

The characteristic roughness height of the bed ( $K_s$ ) was assumed to be  $3.5 D_{84}$  (Hey, 1979). Normalized grain shear stress ( $\phi'$ ) is the ratio of the grain shear stress ( $\tau'$ ) to the critical shear stress for particle mobilization ( $\tau_c$ ). When  $\phi'$  is equal to 1 the bed material begins to mobilize (point of incipient motion), and substantial sediment transport occurs when  $\phi' > 1.5$  (Mussetter et al., 2001). The concept of equi-mobility, as advanced by Parker and Andrews (Parker et al., 1982; Andrews, 1984), shows that at  $\phi' > 1.5$  all material up to about 5 times the median size can be transported by the flow.

The incipient motion analysis was conducted using the reach-averaged hydraulic results and the representative subreach bed material gradations. It should be noted that the incipient motion analysis was carried out only for the median grain size and does not represent the full range of sizes that make up the subreach bed material (i.e., flows that are not capable of creating incipient conditions for the median size may be capable of mobilizing the finer bed material). Results from the incipient motion analysis (**Figure 3.1**) indicate that, in general, incipient conditions ( $\phi' = 1$ ) occur in subreaches with bed material that has a median grain size of coarse sand to very fine gravel ( $D_{50} < 4$  mm) at about the 1-percent exceedence discharge; in subreaches where the median bed-material grain size is greater than very fine gravel ( $D_{50} > 4$  mm), incipient conditions occur very infrequently. Subreaches that are not included in this general statement are Subreaches 6.1 and 10.2. In Subreach 6.1, the hydraulic energy is insufficient to mobilize the relatively fine sediment over the range of modeled flows due to the high frequency of large woody debris jams. Flows on the order of the 10-percent exceedence discharge mobilize sediments in Subreach 10.2, but higher flows are affected by downstream

backwater, and therefore, do not mobilize the bed material. Above Hale Creek (Subreaches 1.1 through 1.3), incipient conditions occur at about the 10-percent exceedence discharge.

Except in Subreaches 6.1, 6.2, and 10.2, significant sediment transport ( $\phi' > 1.5$ ) occurs in the subreaches with a median grain size of less than 4 mm at moderate flows that are greater than the 1-percent exceedence discharge. Significant bed material transport rarely occurs in the coarse-grained subreaches with a median grain size of greater than 4 mm.

## 4. SEDIMENT-TRANSPORT CAPACITY

To compute annual bed-material transport volumes, sediment-transport capacity rating curves were developed for each of the subreaches using the subreach-averaged hydraulics, the representative subreach bed-material gradations and appropriate sediment-transport formulae. The sediment rating curves were also used with the flow-duration data to estimate the effective (channel-forming) discharge (Biedenharn et al., 2001).

### 4.1. Selection of Sediment-Transport Formula

Selection of the sediment-transport formula used to compute the bed material transport capacity sediment-rating curves for the individual subreaches was based on the range of bed material sizes, hydraulic characteristics within the study reach, and previous experience with similar channels. Initially, the U.S. Army Corps of Engineers SamAid program, Version 4.0 (Ayres, 2003), was used to evaluate the applicability of the various sediment-transport formulae. SamAid is part of the SAMwin software and is a tool that provides guidance in the selection of sediment-transport formulae. The software compares input sediment size ( $D_{50}$ ) and hydraulic information (main channel velocity, hydraulic depth, topwidth and energy grade) to a database of rivers (Brownlie, 1981) that have sufficient sediment data to determine an appropriate sediment transport function. The initial screening indicated that a range of functions would be most applicable to the varying hydraulic and bed material characteristics in the various subreaches of the North Branch Root River. These equations include the Yang (sand and gravel) (Yang, 1972), Meyer-Peter and Müller (MPM, 1948), Laursen (Madden) (Madden, 1993), Laursen (Copeland) (Copeland and Thomas, 1989), Parker (Parker, 1990), and Schocklitsch (Schocklitsch, 1930) equations. Results from the comparison of the North Branch Root River data to the SamAid (measured) data indicate that the Yang (sand and gravel) equation was the best match in 11 of the 28 subreaches and either the best or second best match in all 28 subreaches over the range of flows that are exceeded between 50 and 1 percent of the time. Based on this comparison and previous experience with similar rivers, the Yang (sand and gravel) equation was selected for use in the majority of the study reach.

The Yang (sand and gravel) equation is a relationship that relates the concentration of the bed material discharge as a function of the rate of energy dissipation in the flow using dimensional analysis and the unit stream power concept. The basic form of Yang's equation is:

$$\log C_s = M + N \log \frac{VS}{\omega} \quad (4.1)$$

where  $C_s$  = total bed-material concentration in ppm  
 $V$  = flow velocity  
 $S$  = slope  
 $\omega$  = fall velocity of sediment

M, N = dimensionless parameters related to the flow

The values of M and N were determined by regression analysis of field and laboratory data. Field and laboratory data range from 0.9 to 7.01 mm for particle size ( $d_s$ ), 0.037 to 49.9 feet for water depth, and from 0.000043 to 0.0031 for water-surface slope.

The dimensionless relationships for total sediment concentration are:

For sand:

$$\log C_s = 5.435 - 0.286 \log \frac{\omega d_s}{\nu} - 0.457 \log \frac{V_*}{\omega} + 1.799 - 0.409 \log \frac{\omega d_s}{\nu} - 0.314 \log \frac{V_*}{\omega} + \log \frac{VS}{\omega} \frac{V_c S}{\omega} \quad (4.2)$$

For gravel:

$$\log C_s = 6.681 - 0.633 \log \frac{\omega d_s}{\nu} - 4.816 \log \frac{V_*}{\omega} + 2.784 - 0.305 \log \frac{\omega d_s}{\nu} - 0.282 \log \frac{V_*}{\omega} + \log \frac{VS}{\omega} \frac{V_c S}{\omega} \quad (4.3)$$

where  $\nu$  = kinematic viscosity

$V_*$  = shear velocity given by:

$$V_* = \sqrt{gRS} \quad (4.4)$$

where  $g$  = acceleration due to gravity

$R$  = hydraulic depth of the main channel

In the above equations, the dimensionless critical velocity ( $V_c$ ) is given by:

$$\frac{V_c}{\omega} = \frac{2.5}{\log \frac{V_* d_s}{\nu} - 0.06} + 0.66 \quad \text{for } 1.2 < \frac{V_* d_s}{\nu} \quad (4.5)$$

and

$$\frac{V_c}{\omega} = 2.5 \quad \text{for } \frac{V_* d_s}{\nu} \geq 70 \quad (4.6)$$

The sand equation is applicable for sizes up to 2 mm and the gravel equation is applicable for sizes between 2 and 10 mm.

Since the Yang equation (Equations 4.1 through 4.6) is based on the concept of unit stream power ( $VS$ ), computed concentrations are very sensitive to the slope of the hydraulic energy gradient. In the upstream subreaches (Subreaches 1.1 through 1.3), the bed slope is approximately 0.005 and the resulting energy slopes do not fall within the range of slopes that were used in the development of the coefficients in the Yang equation; thus, the Yang equation may not accurately predict sediment concentrations in these subreaches. Indeed, computed sediment concentrations based on the Yang equation were unreasonable in these subreaches, with concentrations as high as 950 ppm at 3 cfs, as high as 2,560 ppm at 36 cfs, and as high as 7,200 ppm at the 100-year event (700 cfs). Because significant portions of the bed material in these subreaches consist of coarse material that is capable of hiding the finer material in the

bed matrix, the Wilcock and Crowe (2003) equation was selected for use in Subreaches 1.1 through 1.3. The Wilcock and Crowe equation was developed through a series of experiments designed specifically to study the hiding effects and resulting transport of sand/gravel mixtures. The Wilcock and Crowe equation computes the bed material load per unit width by size fraction ( $q_{bi}$ ) as:

$$q_{bi} = \frac{W_i^* F_i V_*^3}{(s-1)g} \quad (4.7)$$

where  $V_*$  = shear velocity (Equation 4.4)  
 $s$  = ratio of sediment to water density  
 $F_i$  = fraction of size  $i$  on the bed surface  
 $g$  = acceleration due to gravity, and

$$W_i^* = 0.002\phi^{7.5} \quad \text{for } \phi < 1.35$$

$$W_i^* = 14 \left( 1 - \frac{0.894}{\phi^{0.5}} \right)^{4.5} \quad \text{for } \phi \geq 1.35 \quad (4.8)$$

where  $\phi$  is the ratio of the bed shear stress to the reference shear stress. The reference shear stress is based on the fraction of sand that is present in the bed material and an experimentally derived hiding function.

The Wilcock and Crowe equation was also used to estimate the mixed sand and gravel sediment loading from Whitnall Park Creek due to the hiding effects of the coarse material in this tributary (pebble counts WPC1 and WPC2, Figure 2.5).

## 4.2. Sediment-transport Capacity Rating Curves

Subreach-averaged hydraulic data and the representative subreach gradations were used as input to the Yang equation (or the Wilcock and Crowe equation) to develop sediment-transport capacity rating curves for each of the subreaches (**Figures 4.1a through 4.1c**). To develop the upstream sediment supply to Subreach 1.1, a sediment-rating curve was developed using the Wilcock and Crowe (2003) equation based on the representative subreach gradation for Subreach 1.1 and hydraulic conditions that were estimated using a short hydraulic model of the North Branch Root River upstream from the South 124<sup>th</sup> Street culvert (see Technical Memorandum: Hydraulics). Sediment rating curves were not developed for the subreaches with bed material that is primarily coarse gravel ( $D_{50} > 16$  mm) (Subreaches 3.1, 3.2, 4, 5.1 and 9.4) since this size of bed material is outside the range of applicability for the Yang equation. The sediment-transport analysis in these coarser bed-material subreaches is discussed in Chapter 5.

The primary tributaries to the North Branch Root River (upstream from the confluence with the Root River Canal) include:

- Hale Creek
- 104<sup>th</sup> Street Ditch
- Wildcat Creek

- Whitnall Park Creek
- Dale Creek
- The unnamed tributary below West Loomis Road
- Legend Creek
- East Branch Root River
- Tuckaway Creek
- Ryan Creek

Field observations indicated that many of these tributaries deliver insignificant amounts of sediment to the North Branch Root River. Numerous large woody debris jams trap the majority of bed-material load in the downstream portion of Wildcat Creek (**Figure A.17**). The downstream segments of Dale Creek and the unnamed tributary flow through low-gradient swamps that trap the majority of the upstream sediment load (**Figure A.18**). Under current conditions, Ryan Creek delivers very little if any sediment to the North Branch Root River because of the extensive beaver dams in the lower reaches (**Figure A.19**).

Sediment-rating curves were developed for the remainder of the tributaries that contribute significant amounts of sediment to the North Branch Root River (**Figure 4.2**). Hydraulic characteristics were estimated based on normal-depth conditions and surveyed cross sections at the mouths of Hale Creek, 104<sup>th</sup> Street Ditch, Whitnall Park Creek, and East Branch Root River. The hydraulic data and the tributary gradation curves (Figure 2.5) were used as input to the Yang equation for Hale Creek, 104<sup>th</sup> Street Ditch and East Branch Root River, and as input to the Wilcock and Crowe (2002) equation for Whitnall Park Creek. Since no channel survey information was available to estimate hydraulic conditions on Legend Creek and Tuckaway Creek, sediment loading from these tributaries was estimated by fitting a power function to the sediment-rating curve for the East Branch Root River. The power function fit was made using an exponent of 1.5, a typical value for gravel-bed streams similar to these tributaries (Parker, 1990). The rating curve for Legend Creek and Tuckaway Creek is shown in Figure 4.2.

As expected, significant variability is indicated by the sediment rating curves for the various subreaches in the North Branch Root River. Generally, low transport rates are indicated in subreaches with relatively coarse bed material or in subreaches that do not have the hydraulic energy to transport sediment; higher transport rates are indicated in subreaches with finer bed material. In many of the subreaches, a reversal in the sediment rating curves is indicated, where the sediment-transport capacity increases with increasing discharge at lower flows but decreases with increasing discharge at higher flows. This reversal typically occurs in areas where backwater conditions result in reduced energy slopes at high flows. Subreaches with significant reversal of the sediment-rating curve include Subreach 2.3 (high-flow backwater conditions upstream from West Beloit Road), Subreach 3.2 (high-flow backwater conditions upstream from the constructed ponds), Subreach 5.2 (high-flow backwater conditions upstream from South 76<sup>th</sup> Street), Subreaches 6.1 and 6.2 (high-flow backwater conditions upstream from West Rawson Street), and Subreach 10.2 (high-flow backwater conditions due to the downstream constriction of the floodplain by the bounding terraces [see Technical Memorandum: Geomorphology]).

### 4.3. Annual Sediment-transport Volumes

The sediment-rating curves were used to compute the average annual bed-material volume that each subreach is capable of transporting, by size fraction, using estimated mean daily flow characteristics (**Figure 4.3**). The mean daily flow-duration curves shown in Figure 4.3 were developed as part of the hydrologic analysis (see Technical Memorandum: Hydrology). Average annual bed-material capacity volumes were also computed using the tributary sediment-rating curves and the mean daily flow-duration curves for the tributaries (**Figure 4.4**). Similar to the sediment-rating curves, significant variability is indicated among the computed annual transport volumes (**Figure 4.5**). The volume and size of sediment that each subreach is capable of transporting is dependent on the size of the bed material, the hydraulic conditions and the magnitude and frequency of the flows. A general trend of increasing annual sediment load with increasing drainage area is indicated, despite the variability in bed material size. In some subreaches, it is the hydraulic conditions that control the sediment loading. For example, the computed load in Subreach 1.1 is relatively high due to the high-energy gradients that occur over the range of modeled discharges, while low energy gradients in Subreach 3.3 result in low transport rates despite the relatively small bed-material size. In some subreaches, the grain size is the dominant factor in the capacity calculations (i.e., the relatively high sediment load in Subreach 3.4 is consistent with the mostly sand material available in the bed.)

### 4.4. Effective Discharge

The concept of effective discharge, as advanced by Wolman and Miller (1960), related the frequency and magnitude of various discharges to their ability to do geomorphic work by transporting sediment. They concluded that events of moderate magnitude and frequency transported the most sediment over the long-term, and that these flows were the most effective in forming and maintaining the planform and geometry of the channel. Andrews (1980) defined the effective discharge as “*the increment of discharge that transports the largest fraction of the annual sediment load over a period of years.*”

Alluvial rivers adjust their shape in response to flows that transport sediment, and numerous authors have attempted to relate the effective discharge to the concepts of dominant discharge, channel-forming discharge and bankfull discharge, and it is often assumed that these discharges are roughly equivalent and correspond to approximately the mean annual flood peak (Benson and Thomas, 1966; Pickup, 1976; Pickup and Werner, 1976; Andrews, 1980, 1986; Nolan et al., 1987; Andrews and Nankervis, 1995). Quantification of the range of flows that transport the most sediment provides useful information to assess the current state of adjustment of the channel, and to evaluate the potential effects of increased discharge and sediment delivery to channel behavior. Although various investigators have used only the suspended-sediment load and the total sediment load to compute the effective discharge, the bed-material load should generally be used when evaluating the linkage between sediment loads and channel size because it is the bed-material load that has the most influence on the morphology of the channel (Schumm, 1963; Biedenharn et al., 2000).

For purposes of this study, the effective discharge was computed by dividing the range of flows into 30 logarithmic classes and then computing the total quantity of bed material load transported by the flows within each class. An example of the effective discharge is shown in **Figure 4.6**. The effective discharge was not calculated in the subreaches with coarse bed material (Subreaches 3.1, 3.2, 4, 5.1 and 9.4) and in the low-gradient reach below West Loomis

Road (Subreach 6.1), since the incipient motion analysis indicates that the bed material in these subreaches is very rarely mobilized.

The effective discharge calculations (**Figure 4.7**) indicate that the computed effective discharge is generally greater than the 1-percent exceedence discharge in the subreaches upstream from West Loomis Avenue, and approximates the 1-percent exceedence discharge in the downstream subreaches. These results are consistent with the evaluation of bankfull flows. As discussed in the Geomorphology Technical Memorandum, the bankfull discharge in the upstream subreaches is equal to or greater than the 2-year event, while bankfull flows in the downstream subreaches tend to be much less (about the 1-percent exceedence discharge). Compared to the effective discharge in other upstream subreaches, the computed effective discharge in Subreach 2.4 is relatively low (38 cfs, or about the 2.9-percent exceedence discharge). However, the effective discharge histogram (**Figure 4.8**) indicates that significant incremental sediment loads also occur in the 81-cfs discharge class (about the 0.9-percent exceedence discharge). In Subreach 10.2 the effective discharge is only about 360 cfs (about the 1.6-percent exceedence discharge) because of the reversal in the bed-material sediment rating curve (Figure 4.1c), an artifact of backwater effects at higher discharges resulting from the downstream terrace constriction.

## 5. SEDIMENT-TRANSPORT ANALYSIS—EXISTING CONDITIONS

The sediment-continuity analysis was performed by comparing the annual bed-material transport capacity of each subreach (Figure 4.5) to the bed-material supply from the upstream river and local tributaries within the subreach (**Figure 5.1**). Where the transport capacity of a particular subreach exceeds the supply, the channel will respond by either degrading (i.e., channel downcutting) or coarsening its bed material, and where the supply exceeds the capacity, the channel will respond by aggrading or fining its bed material. Significant amounts of downcutting or aggradation can also lead to lateral instability that is not directly addressed by the continuity analysis.

For the coarse-grained subreaches with bed material composed of mostly coarse gravel ( $D_{50} > 16$  mm) (Subreaches 3.1, 3.2, 4, 5.1, and 9.4), the incipient-motion analysis (Chapter 3) was used to evaluate the potential for aggradation or degradation, since bed material sediment rating curves (and therefore annual sediment volumes) were not computed in these areas because of the infrequency of bed-material mobilization. In each of these subreaches, the incipient-motion analysis indicates that the median grain size is mobilized very infrequently (Figure 3.1), indicating the potential for degradation is unlikely. To evaluate the potential for aggradation in these subreaches, an assessment of the ability of the flows to transport the finer-grained material from upstream sources was carried out. If the transport capacity of the supplied material exceeds the upstream supply, the supplied material is passed through the subreach as throughput, if the upstream supply exceeds the transport capacity of this material, then deposition (aggradation) is indicated.

This assessment was carried out by computing the transport capacity of these subreaches using the subreach-averaged hydraulic conditions and the gradation of the material that is being supplied by upstream sources. This gradation was estimated using the size distribution of the computed average annual capacity of the next upstream subreach with relatively fine-grained bed material ( $D_{50} < 10$  mm) (Figure 4.5). For example, the gradation of the annual capacity of

Subreach 2.4 was used to evaluate the transport capacity of the supplied load to Subreaches 3.1 and 3.2, since the bed material in these subreaches is coarse-grained.

In each of the coarse-grained subreaches, the computed transport capacity exceeds the upstream supply volume, indicating that the upstream sediment supply is passed as throughput to the next downstream subreach (Figure 5.1). The bed material load supplied to Subreaches 3.1 and 3.2 from 104<sup>th</sup> Street Ditch is also passed through these two subreaches, since the transport capacity (based on the gradation of the tributary loading) exceeds the tributary supply. However, it is likely that aggradation will occur in Subreach 5.1, since the relatively coarse-grained tributary supply from Whitnall Park Creek exceeds the transport capacity of this sized material.

During the field reconnaissance, numerous natural or man-made grade-control structures were observed that limit the potential for degradation, which results in upstream sediment load throughput conditions in some subreaches. In Subreach 1.1, a significant portion of the channel bed is protected with riprap (**Figure A.20**), and the concrete sill below West Lincoln Avenue (**Figure A.21**) provides grade control. Therefore, the upstream sediment supply was passed through Subreach 1.1 and was used as the supply to Subreach 1.2 in the sediment-continuity analysis. Similar sediment throughput conditions were observed in the vicinity of the gravel pits (Subreach 7), where a constructed boulder grade-control structure (**Figure A.22**), numerous gravel riffles (**Figure A.23**), and localized boulder clusters (**Figure A.24**) minimize the potential for downcutting. The transport capacity volume of Subreach 6.2 was, therefore, used as the upstream supply to Subreach 8.1. Throughput conditions in Subreaches 1.1 and 7 were verified by comparing the transport capacity of the upstream load to the supply volume (Figure 5.1).

Results from the sediment-continuity analysis (**Figure 5.2**) indicate that, in general, annual volumes of bed material that are stored or depleted from each subreach tend to be relatively small under existing hydrologic conditions. (The average annual aggradation/degradation volumes were converted into annual changes in mean bed elevation using the average width and length of each subreach.) Except for Subreach 5.1, no aggradation or degradation is indicated in the throughput subreaches (Subreaches 1.1, 3.1, 3.2, 4, 7 and 9.4) since the upstream sediment load is passed to the next downstream subreach, and the flows are not capable of mobilizing the bed material within the subreach or sufficient grade-control exists to limit degradation. In Subreach 5.1, the upstream supply is passed through the subreach, but slight aggradation occurs due to deposition of coarse sediments from Whitnall Park Creek. In the remainder of the subreaches, the average annual change in bed elevation is less than about 0.1 feet. The most strongly aggradational subreaches (about 0.1 ft/yr) are Subreach 2.1 due to significant sediment loads from both the upstream North Branch Root River and Hale Creek, Subreach 5.2 due to the sediment-trapping effects of the numerous large woody debris jams, and Subreaches 8.4 and 9.1 due to large tributary loads from East Branch Root River that consist of moderately coarse material. The largest degradation depths are indicated in Subreach 1.2 due to the steep channel gradient, and in Subreaches 3.4 and 10.2 due to the relatively fine-grained and highly erodible finer sediments present in the bed. Moderate degradation (about 0.04 ft/yr) is also indicated in Subreaches 8.2 and 9.3.

The sediment-continuity analysis was validated, to the extent possible, using field observations and comparative thalweg profiles (**Figure 5.3**). The thalweg profiles were developed using information from Harza (1966) and from the 2005/2006 MMSD cross-section surveys (see Technical Memorandum: Surveying). Although a comparison of the thalweg profiles from 1966 and 2006 does not provide insight into current rates of aggradation or degradation, general trends are evident. It should also be noted that the 1966 thalweg profile does not have the

resolution of the 2006 survey profile and, therefore, the indicated change in bed elevation in some locations could be exaggerated.

Comparison of the computed aggradation/degradation trends with the field observations (**Table 5.1**) indicates that the results from the sediment-continuity analysis are reasonable. Results from the sediment-continuity analysis are also generally consistent with the trends indicated by the comparative thalweg profiles. In some locations, the predicted minor increase in bed elevation does not agree with the degradation indicated by the comparative profiles (Subreach 2.1 and Subreaches 8.4 through 9.2), possibly the result of recent channel adjustments to increased sediment loading from Hale Creek and East Branch Root River. This could also be a result of initial channel responses to urbanization that occurred prior to the mid-1980s followed by less noticeable responses to continued urbanization over the past two decades.

## 6. SEDIMENT-TRANSPORT ANALYSIS—FUTURE CONDITIONS

The sediment continuity analysis was revised to evaluate the effects of continued urbanization in the watershed by re-computing the average annual transport capacity volumes using the mean daily flow duration curves for 2020 conditions (**Figures 6.1 and 6.2**) (see Technical Memorandum: Hydrology). The annual bed material transport capacity volumes (**Figure 6.3**) under future conditions are slightly larger than the volumes under existing conditions in the North Branch Root River (about 15 percent) due to the increases in flow. In the East Branch of the Root River, where the transport capacity increases by nearly 73 percent from 1,040 tons/yr under existing conditions to 1,790 tons/yr under future conditions due to increased flows from significant future urbanization in the contributing watershed. A comparison of the computed annual bed-material transport capacity with the upstream and tributary supply volumes was carried out using the same procedures and assumptions that were used for the existing conditions sediment-continuity analysis (including the evaluation of throughput loads). The resulting volumes of aggradation and degradation and the corresponding change in bed elevation under future conditions indicate that the general trends of erosion and sedimentation are similar to those observed under existing conditions, but the magnitude of the volume of material eroded or deposited in each subreach is slightly larger (**Figure 6.4**). Annual degradation volumes increase by an average of about 15 percent, with the largest increase in Subreach 9.3 due to the hydrologically driven increase in bed-material transport capacity. Annual aggradation volumes increase by about 38 percent, and the largest increases occur in the subreaches below Legend Creek, East Branch Root River, and Tuckaway Creek (Subreaches 8.3, 8.4, and 9.2) that result from the increased flows and sediment loads from these tributaries.

Under future (2020) conditions, the corresponding changes in bed elevation are slightly larger than under existing conditions, but are still relatively small. The largest rates of aggradation and degradation generally occur in the same locations that are indicated by the existing conditions analysis. The largest rates of aggradation occur below Hale Creek (Subreach 2.1), above South 76<sup>th</sup> Street (Subreach 5.2), and between Legend Creek and Tuckaway Creek (Subreaches 8.3 through 9.2). The significant increase in sediment loads from the East Branch of the Root River suggests that the reach below this tributary (Subreach 8.4) will be the most strongly aggradational under future conditions, but that the rates will remain relatively low (less than 0.15 ft/yr). Similar to the results from the existing conditions analysis, the largest rate of degradation is indicated in Subreach 3.4 (about 0.13 ft/yr).

## 7. EVALUATION OF LATERAL EROSION POTENTIAL

Because the observed rates and magnitudes of bank erosion in the project reach of the North Branch Root River are relatively small, and because analytical methodologies do not allow for detailed predictions of the rate of bank erosion, a quantitative analysis of the potential for lateral erosion was not conducted. Although the Bank Energy Index (BEI) (Mussetter and Harvey, 1995) concept could be used to provide an index for lateral erosion, this concept is only useful when a baseline condition has been developed for comparison with BEI values from alternate conditions. A qualitative analysis of the potential for lateral erosion is more appropriate for this study, and was carried out using the results from the bed material sediment-continuity analysis, field observations, and the geomorphic analysis (see Technical Memorandum: Geomorphology).

Bank erosion generally occurs by one of three primary modes: (1) mass slope failure due to geotechnical instability, (2) surficial weathering of cohesive bank materials, and (3) grain-by-grain erosion of noncohesive materials due to the shearing action of the flow along the bank. In all three cases, the duration and magnitude of flows through the reach can affect the erosion potential. Bank erosion in the North Branch Root River and its tributaries currently occurs primarily due to surficial weathering of the cohesive bank materials and by grain-by-grain erosion, although some locations, in the more deeply incised downstream subreaches, are affected by slope failures.

Mass slope failures result from a variety of processes, including oversteepening of the bank due to channel incision or local scour, undercutting of the bank, and by excess pore-water pressure that weakens the strength of the bank material. Bank heights in the North Branch Root River and its tributaries tend to be too low for mass failures to occur, except in the downstream subreaches (Subreaches 10.1 and 10.2; **Figures A.25 and A.26**). However, based on the sediment-continuity analysis, continued incision upstream from Hale Creek (Subreaches 1.2 and 1.3), above West Grange Avenue (Subreach 3.4), below Ryan Creek (Subreach 10.2), and to a lesser extent upstream from Legend Creek (Subreach 8.2) and below Tuckaway Creek (Subreach 9.3), could lead to greater bank heights that would be more susceptible to bank erosion by mass failure. Surficial weathering of the bank materials (**Figures A.27 and A.28**) could be exacerbated by increased flow fluctuations (wetting and drying cycles) associated with future urbanization, but bank erosion caused by this process occurs at relatively slow rates. The mechanism of bank erosion that is most heavily influenced by urbanization in the North Branch Root River watershed is grain-by-grain erosion (**Figure A.29**), since this mechanism is directly related to the magnitude and duration of shearing flows. Entrainment of bank materials is often linked to channel aggradation, especially where deposition of bed material occurs in the form of a bar, resulting in concentrated flows along one or both banks. These concentrated flows tend to have higher shearing forces than flows that are uniformly distributed over the width of the channel, and therefore, increase the potential for bank erosion. The largest potential for increased lateral migration occurs in subreaches that are the most aggradational (Subreaches 2.1, 3.3, 5.2, and 8.4 through 9.2).

Regardless of the mechanism of bank erosion, based on a comparison of the channel locations in 1950 and 1956 with the current channel locations, the rates of lateral erosion along the North Branch Root River are very low. In all of the subreaches, bank erosion is at least somewhat limited by significant tree root reinforcement of the banks (**Figures A.30 and A.31**). In some subreaches, fine-grained lateral accretion deposits are located on the channel banks upstream

of large woody debris jams (**Figure A.32**), and these limit the potential for further bank erosion. Recommendations for treating and prioritizing areas where bank erosion could impact infrastructure are presented in the Management Recommendations Technical Memorandum.

## 8. SUMMARY AND CONCLUSIONS

The sediment-transport analysis that is described in this technical memorandum was performed to provide MMSD with a tool for evaluating the existing vertical and lateral stability of the North Branch Root River, and for assessing the impacts of altered hydrologic conditions associated with anticipated future urbanization on channel stability. The results from this analysis can be used by the District to aid in flood management and other planning purposes.

The sediment-continuity analysis was conducted by generating bed-material transport capacity sediment rating curves for 28 subreaches that were defined based on the existing channel characteristics and the locations of channel controls and significant sediment inputs (Figure 1.1). The rating curves were developed using estimates of the subreach-averaged hydraulic conditions (see Technical Memorandum: Hydraulics) and sampled bed-material data. The resulting rating curves were then integrated over the annual flow-duration curves (see Technical Memorandum: Hydrology) for existing and future (2020) conditions to obtain an estimate of the average annual volume of bed material that would be transported through each subreach. These volumes were then compared to the bed-material supply from upstream reaches of the river and local tributaries to assess the relative balance between the transport capacity and supply. Where the transport capacity of a particular subreach exceeds the supply, the channel will typically respond by either degrading (i.e., channel downcutting) or coarsening its bed material, and where the supply exceeds the capacity, the channel will respond by aggrading or fining its bed material.

To aid in the evaluation of sediment continuity, an incipient-motion analysis was carried out to determine the range of discharges that are capable of mobilizing the bed material in each subreach. An effective discharge analysis was also conducted to determine the range of discharges that would be expected to carry the bulk of the annual sediment load. The potential for lateral migration of the channel due to bank erosion was evaluated on a qualitative basis to assess the impacts of increased flows on bank erosion.

The following conclusions can be drawn from the results that were obtained from the sediment-transport analyses:

1. Under existing conditions, the rate and magnitude of bed aggradation or degradation is relatively small, with average changes in bed elevation typically being less than 0.1 ft/yr.
2. Under future (2020) conditions, the trends in aggradation and degradation are similar to those under existing conditions, but the magnitude of change is slightly greater.
3. Tributary sediment supply to the North Branch Root River is significant, primarily due to the relatively coarse nature of the bed material in the primary tributaries.
4. The largest change in aggradation or degradation from existing to future hydrologic conditions occurs downstream from the East Branch Root River, since this tributary is expected to experience the largest increase in runoff due to future urbanization.

5. Injection of coarse-grained material from the tributaries and erosion of coarse-grained banks results in no systematic downstream fining trends (Figure 4.5), as well as local controls that limit channel incision. This significantly impacts sediment continuity in the North Branch Root River.
6. Based on the incipient-motion analysis, the range of average annual mean daily flows do not mobilize significant amounts of sediment in subreaches with locally coarse bed material. Locations with coarse bed material include Subreaches 3.1 and 3.2 (104<sup>th</sup> Street Ditch to the Constructed Ponds) and Subreach 9.4 (above West Ryan Road). At these locations, the upstream sediment load is passed through the subreach, resulting in no change in bed elevation.
7. Results from the effective discharge analysis indicate the range of flows that transport the bulk of the annual sediment load is typically similar to bankfull flows (generally about the 1-percent exceedence discharge on the mean daily flow-duration curve). Although this indicates that the channel size is apparently adjusted to the fine-grained sediment (sand) loading, adjustment of channel size is primarily controlled by locally coarse bed material.

While the above analysis is useful in evaluating current trends in aggradation or degradation, it does not directly quantify long-term changes in mean bed elevation, because the transport capacity will adjust as the channel downcuts or aggrades. Nevertheless, the results provide an indication of general trends in erosion and sedimentation and the likely response of specific areas of the channel to increased flows under urbanized hydrologic conditions. Because the indicated degradation volumes are relatively small, and because continued incision will likely be limited by existing grade control, extensive channel downcutting is not expected in most areas. Similarly, the results from the analysis indicate minimal impacts on increased flooding due to continued aggradation.

## **9. REFERENCES**

- Andrews, E.D., 1980. Effective and Bankfull Discharges of Streams in the Yampa River Basin, Colorado and Wyoming. *Journal of Hydrology*, 46(1980), pp. 311-330.
- Andrews, E.D., 1984. Bed material entrainment and hydraulic geometry of gravel-bed rivers in Colorado. *Geological Society of America Bulletin* 95, March, pp. 371-378.
- Andrews, E.D., 1986. Downstream Effects of Flaming Gorge Reservoir on the Green River, Colorado and Utah. *Geological Society of American Bulletin*, v. 97, August, pp. 1012-1023.
- Andrews, E.D. and Nankervis, J.M., 1995. Effective discharge and the design of channel maintenance flows for gravel-bed rivers. *American Geophysical Union*, v. 89, pp. 151-164.
- Ayres Associates, 2003. SamAid program, Version 4.0. Module of U.S. Army Corps of Engineers, SAMwin Hydraulic Design Package. Version 1.0.
- Benson, M.A. and Thomas, D.M., 1966. A definition of dominant discharge. *Bulletin of the International Association of Scientific Hydrology* 11, pp. 76-80.

- Biedenharn, D.S., Copeland, R.R., Thorne, C.R., Soar, P.J., Hey, R.D., and Watson, C.C., 2000. Effective Discharge Calculation: A Practical Guide. Coastal and Hydraulics Laboratory, U.S. Army Engineer Research and Development Center, Vicksburg, Mississippi, ERDC/CHL TR-00-15, August.
- Biedenharn, David S., Soileau, Rebecca S., Hubbard, Lisa C., Hoffman, Peggy H., Thorne, Colin R., Bromley, Chris C. and Watson, Chester C., 2001. Missouri River – Fort Peck Dam to Ponca State Park Geomorphological Assessment Related to Bank Stabilization. Engineer Research Development Center of the COE, 130 p.
- Brownlie, W.R., 1981. Prediction of flow depth and sediment discharge in open channels. Report No. KH-R-43A, California Institute of Technology, W.M. Keck Laboratory of Hydraulics and Water Resources, Pasadena, California, November.
- Copeland, R.R. and Thomas, W.A., 1989. Corte Madera Creek sedimentation study: numerical model. Technical Report for the U.S. Army Eng. Waterways Experiment Station, 81 p.
- Einstein, H.A., 1950. The bedload function for sediment transportation in open channel flows. U.S. Soil Conservation Service, Tech. Bull. No. 1026.
- Harza, 1966. A comprehensive plan for the Root River Watershed. Prepared for Southeastern Wisconsin Research Planning Commission.
- Hey, R.D., 1979. Flow Resistance in Gravel-Bed Rivers. ASCE, Journal of the Hydraulics Division, v. 105, no. HY4, pp. 365-379.
- Madden, E.B., 1993. Modified Laursen Method for estimating bed-material sediment load. U.S. Army Engineer Waterways Experiment Station, U.S. Army, HL-93-3.
- Meyer-Peter, E. and Müller, R., 1948. Formulas for bed load transport. In Proceedings of the 2<sup>nd</sup> Congress of the International Association for Hydraulic Research, Stockholm, 2: Paper No. 2, pp. 39-64.
- Mussetter, R.A. and Harvey, M.D., 1995. Geomorphic and hydraulic characteristics of the Colorado River, Moab, Utah: Potential impacts on a uranium tailings disposal site. Proc. Conference on Tailings and Mine Waste, '96, Colorado State University, January 16-19, 1996, Balkema, Rotterdam, pp. 405-414.
- Mussetter, R.A., Harvey, M.D., and Zevenbergen, L., 2001. A Comparison of One- and Two-Dimensional Hydrodynamic Models for Evaluating Colorado Squawfish Spawning Habitat, Yampa River, Colorado. In Anthony, D.J., Harvey, M.D., Laronne, J.B., and Mosley, M.P. (eds), *Applying Geomorphology to Environmental Management*, Water Resource Publications, Englewood, Colorado, pp. 361-379.
- Neill, C. R. 1968. Note on initial movement of coarse uniform bed material. Journal of Hydraulic Research. 6:2, pp. 173-176.
- Nolan, K.M., Lisle, T.E., and Kelsey, H.M., 1987. Bankfull discharge and sediment transport in northwestern California. A paper delivered at Erosion and Sedimentation in the Pacific Rim, IAHS Publication No. 165, International Association of Hydrological Sciences, Washington, D.C.

- Parker, G., 1990. The “Acronym” series of Pascal programs for computing bed load transport in gravel rivers. University of Minnesota, St. Anthony Falls Hydraulic Laboratory, External Memorandum No. M-220.
- Parker, G., Klingeman, P.C., and McLean, D.G., 1982. Bed load and size distribution in paved gravel-bed streams. *Journal of the Hydraulics Divisions, American Society of Civil Engineers*, 108(HY4), Proc. Paper 17009, pp. 544-571.
- Pickup, G. and Werner, R.F., 1976. Effects of hydrologic regime on magnitude and frequency of dominant discharge. *Journal of Hydrology*, v. 29, pp. 51-75.
- Pickup, G., 1976. Adjustment of stream channel shape to hydrologic regime. *Journal of Hydrology*, v. 30, pp. 365-373.
- Schoklitsch, A., 1930. *Handbuch des Wasserbaues*. Springer, Vienna (2<sup>nd</sup> ed), English translation by Shulits, S., *The Schoklitsch Bed-load Formula*, Engineering, London, England, June 21, 1935, pp. 644-646 and June 28, 1935, p. 687.
- Schumm, S.A., 1963. A tentative classification of alluvial river channels. U.S. Geol. Survey Circ. 477, 10 p.
- Shields, A., 1936. Application of similarity principles and turbulence research to bed load movement. California Institute of Technology, Pasadena; Translation from German Original; Report 167.
- Wilcock, P.R. and Crowe, J.C., 2003. Surface-based transport model for mixed-size sediment. *ASCE, Journal of Hydraulic Engineering*, v. 129, no. 2, pp. 120-128.
- Wolman, M.G. and Miller, J.P., 1960. Magnitude and frequency of forces in geomorphic processes, *Journal of Geology*, vol. 68, no. 1, pp. 54-74.
- Wolman, M.G., 1954. A method for sampling coarse river bed material, *Transactions of American Geophysical Union*, v.35 (6), pp. 951-956.
- Yang, C.T., 1972. Unit Stream Power and Sediment Transport. *ASCE, Journal of Hydraulic Engineering*, v. 98, no. HY10, pp. 1805-1826.

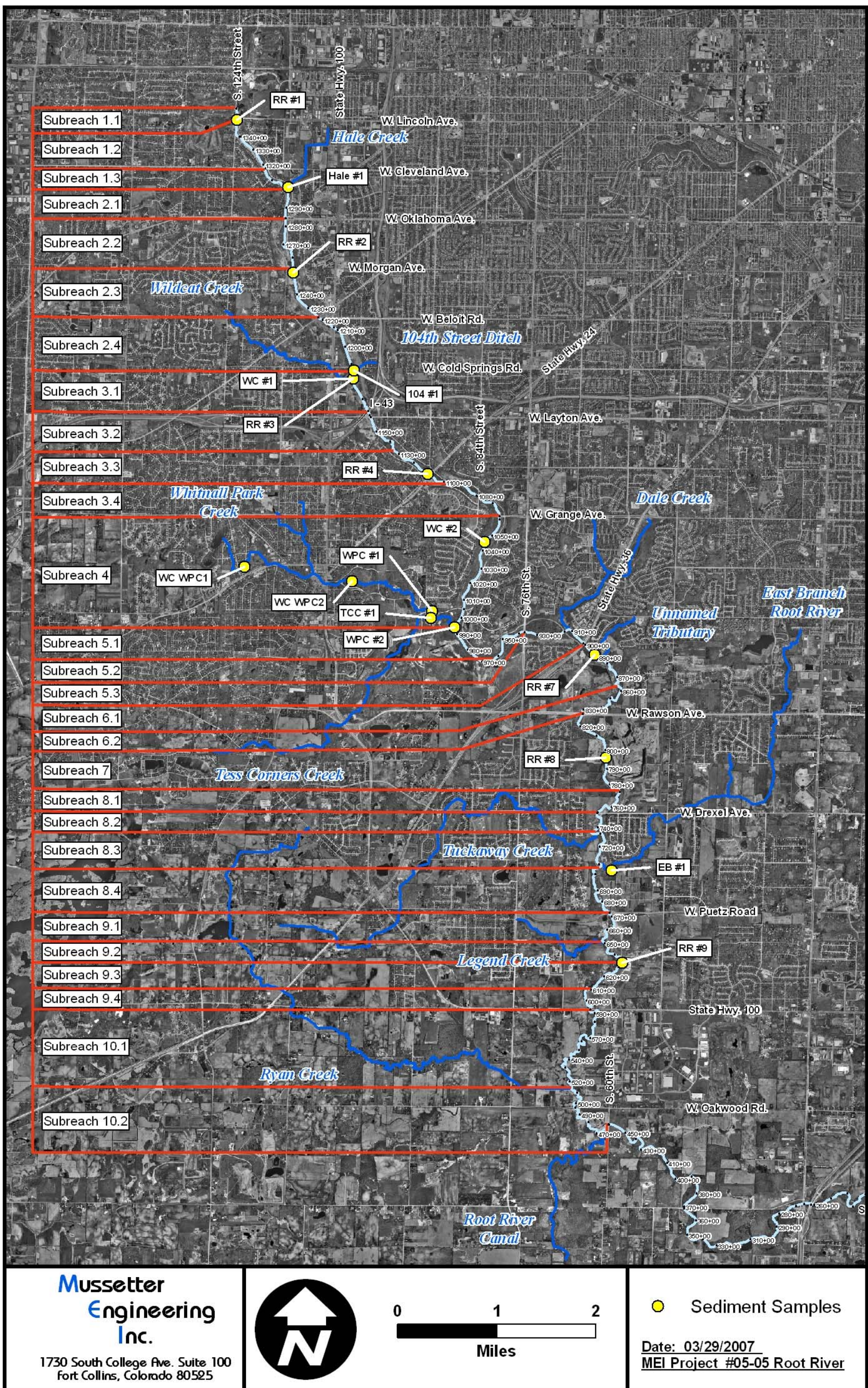


Figure 1.1. Map of the North Branch Root River watershed showing the locations of the primary tributaries. Also shown are the locations of the sediment samples.

Table 2.1. Subreaches used in the sediment-continuity analysis.					
Subreach	Upstream Limit	Downstream Limit	Upstream Station (ft)	Downstream Station (ft)	Length (mi)
1.1	S. 124th St	W Lincoln Ave	135,750	135,175	0.11
1.2	W Lincoln Ave	W Cleveland Ave	135,175	131,774	0.64
1.3	W Cleveland Ave	Hale Creek	131,774	130,018	0.33
2.1	Hale Creek	National Ave	130,018	128,436	0.30
2.2	National Ave	W Morgan Ave	128,436	125,415	0.57
2.3	W Morgan Ave	W Beloit Road	125,415	122,273	0.60
2.4	W Beloit Road	104th St Ditch	122,273	118,515	0.71
3.1	104th St Ditch	I-43	118,515	116,232	0.43
3.2	I-43	Constructed Ponds	116,232	113,300	0.56
3.3	Constructed Ponds	Pedestrian Bridge	113,300	109,400	0.74
3.4	Pedestrian Bridge	W Grange Ave	109,400	106,158	0.61
4	W Grange Ave	Whitnall Park Creek	106,158	99,280	1.30
5.1	Whitnall Park Creek	Ski Hill Pond	99,280	96,320	0.56
5.2	Ski Hill Pond	S. 76th St.	96,320	93,689	0.50
5.3	S. 76th St.	W Loomis Rd	93,689	90,104	0.68
6.1	W Loomis Rd	Below Beaver Dams	90,104	86,300	0.72
6.2	Below Beaver Dams	W Rawson St	86,300	82,785	0.67
7	W Rawson St	D/S Gravel Pit Rch	82,785	77,000	1.10
8.1	D/S Gravel Pit Rch	W Drexel Ave	77,000	74,968	0.38
8.2	W Drexel Ave	Legend Creek	74,968	73,285	0.32
8.3	Legend Creek	East Branch Root River	73,285	70,855	0.46
8.4	East Branch Root River	W Puetz Rd	70,855	67,226	0.69
9.1	W Puetz Rd	Tuckaway Creek	67,226	65,199	0.38
9.2	Tuckaway Creek	Sample RR-9	65,199	63,376	0.35
9.3	Sample RR-9	Sta 610+00	63,376	61,000	0.45
9.4	Sta 610+00	W Ryan Rd	61,000	59,369	0.31
10.1	W Ryan Rd	Ryan Creek	59,369	51,491	1.49
10.2	Ryan Creek	S. 60th St	51,491	46,068	1.03

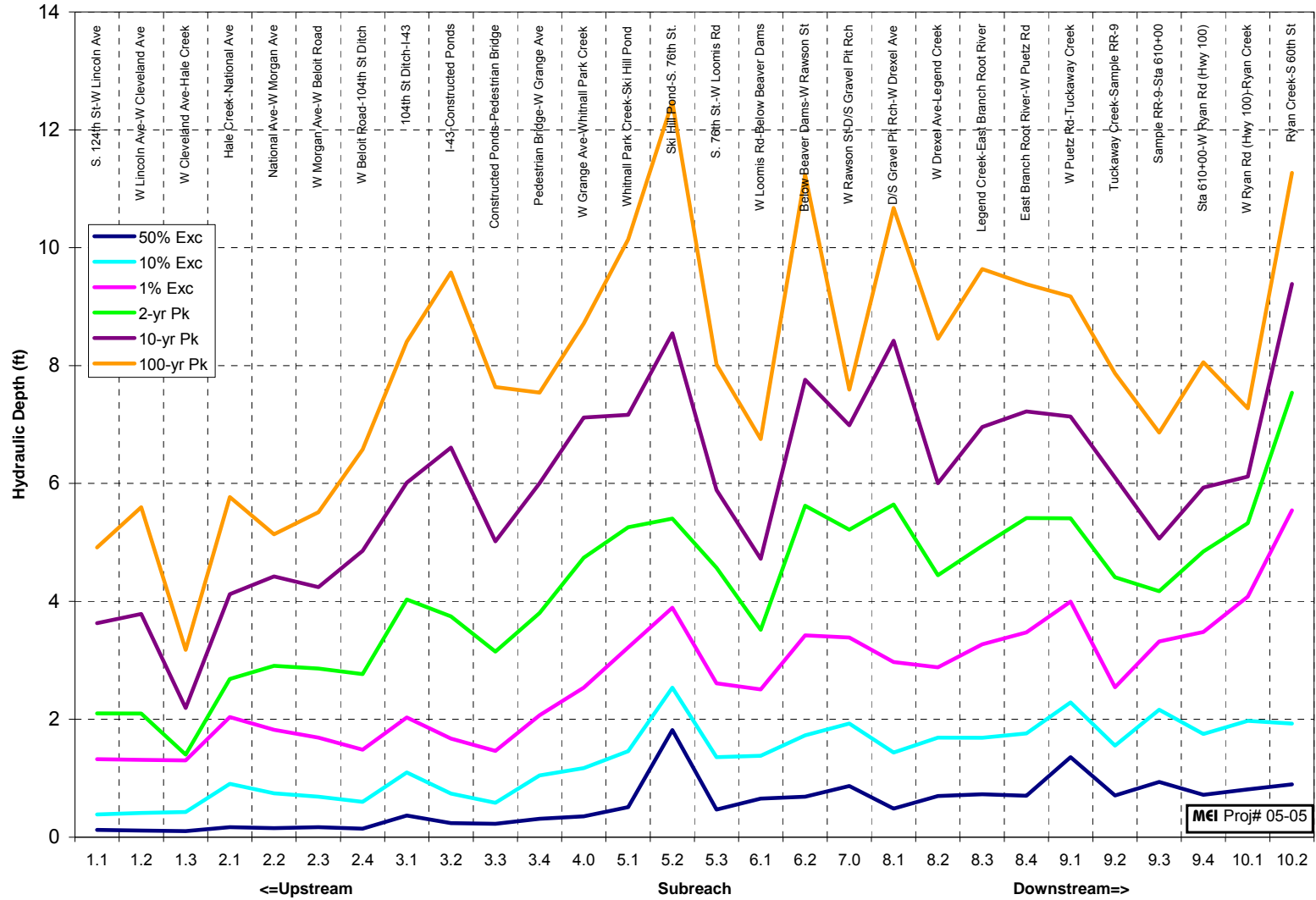


Figure 2.1. Subreach-averaged main channel hydraulic depth profiles for flows ranging from the 50-percent mean daily exceedance flow to the 100-year peak event.

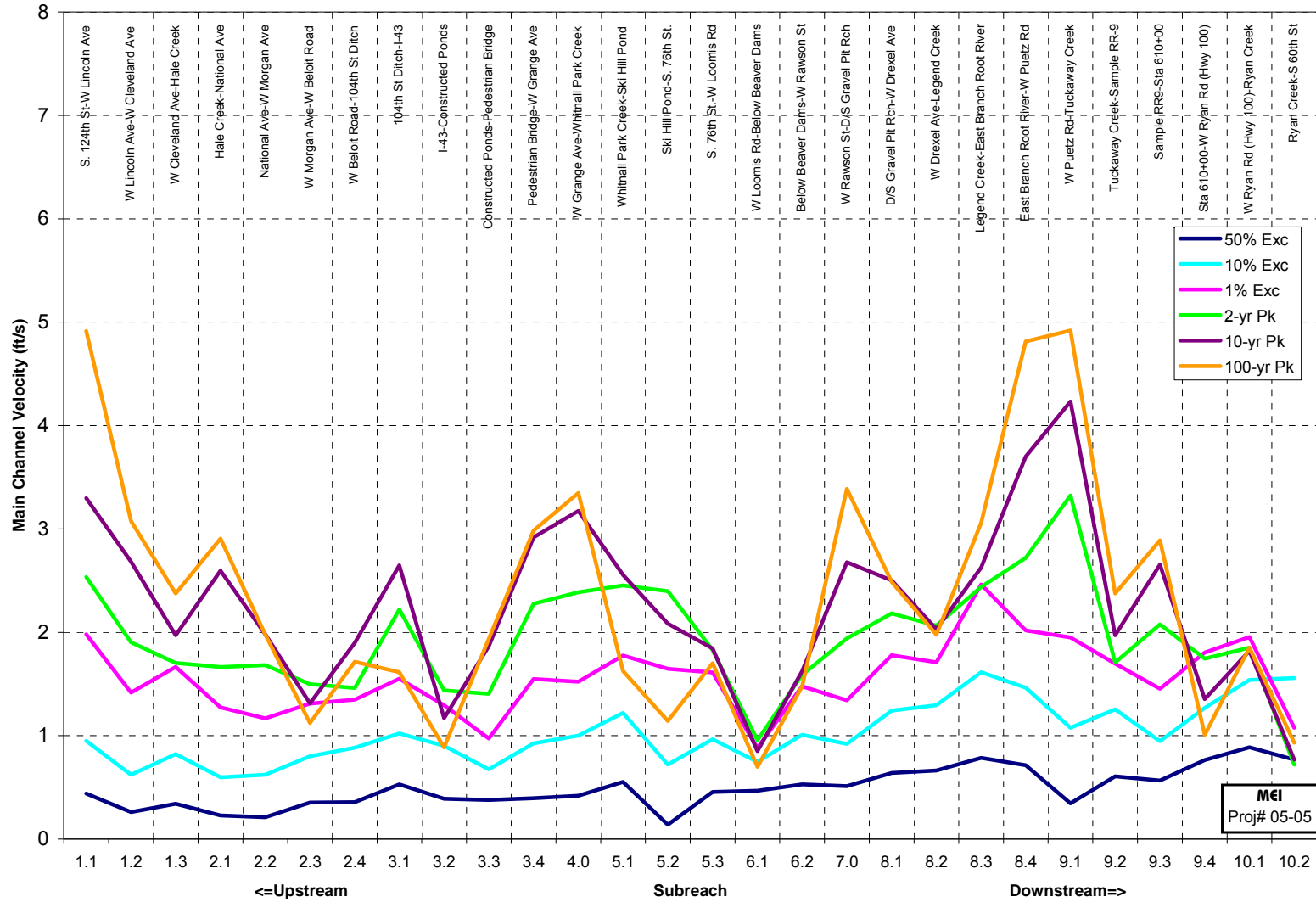


Figure 2.2. Subreach-averaged main channel velocity profiles for flows ranging from the 50-percent mean daily exceedence flow to the 100-year peak event.

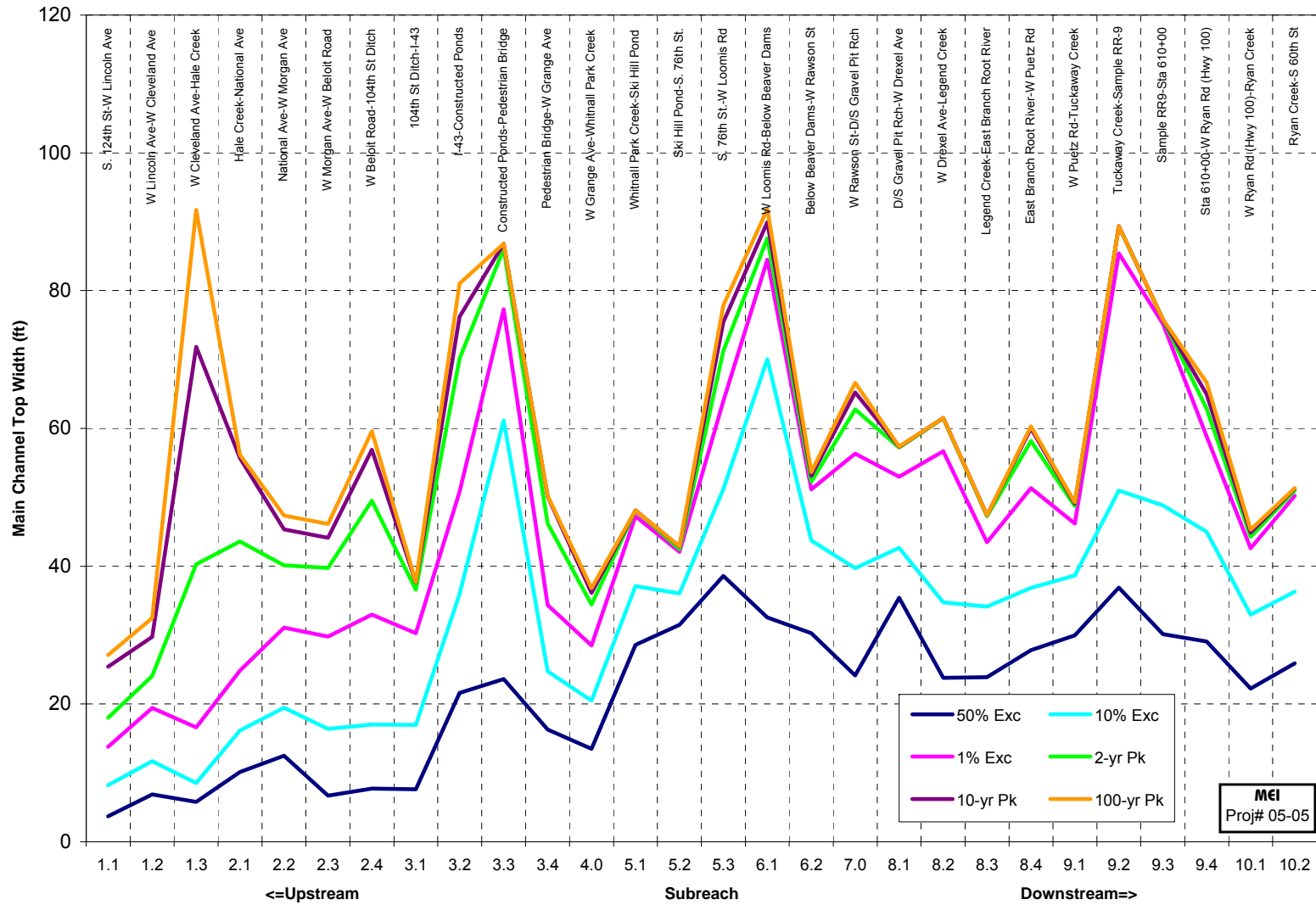


Figure 2.3. Subreach-averaged main channel topwidth profiles for flows ranging from the 50-percent mean daily exceedence flow to the 100-year peak event.

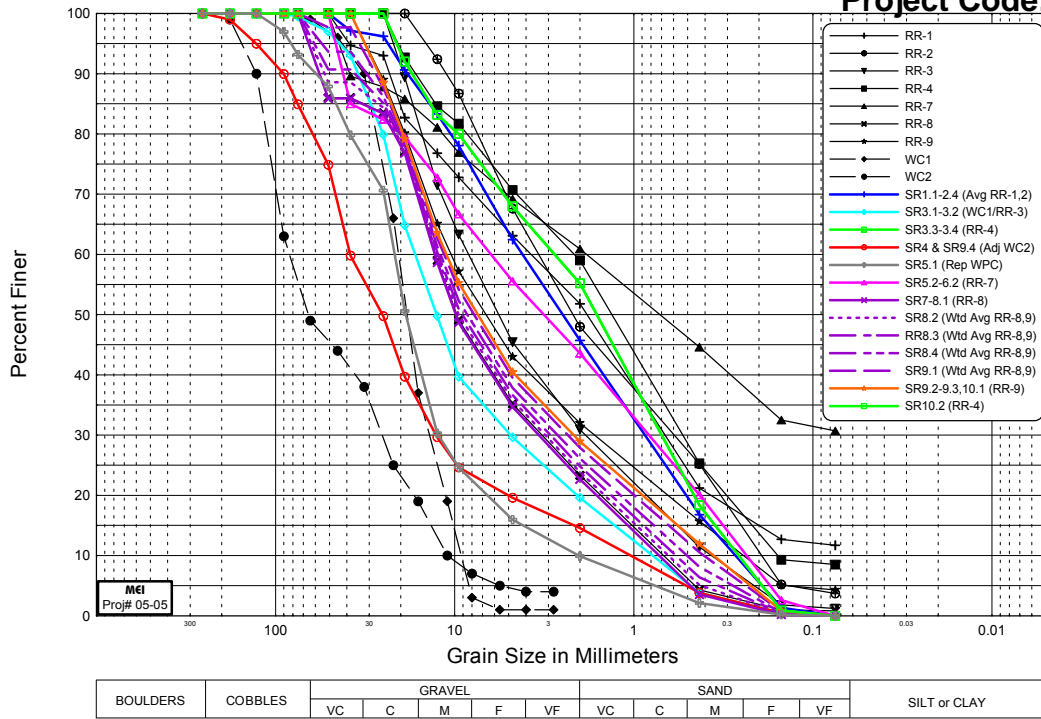


Figure 2.4. Gradation curves for the bulk sediment samples and pebble counts collected on the North Branch Root River. Also shown are the representative subreach gradations used in the sediment-transport analysis.

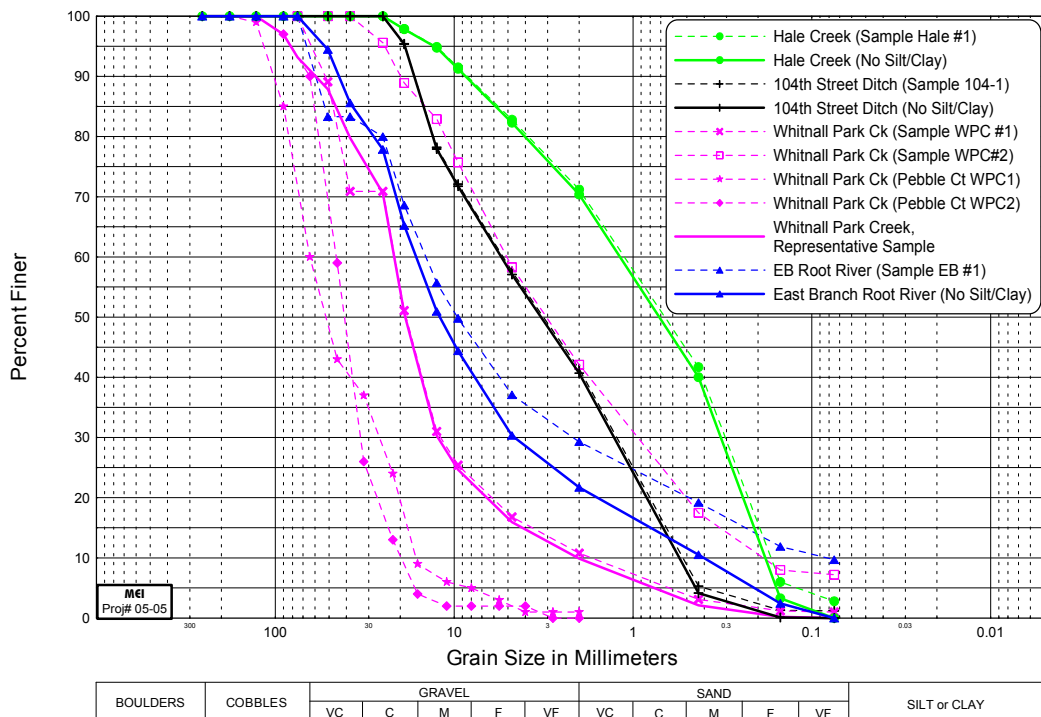


Figure 2.5. Gradation curves for the bulk sediment samples and pebble counts collected on the primary tributaries to the North Branch Root River. Also shown are the representative gradations used in the sediment-transport analysis.

Table 2.2. Summary of representative subreach gradations.				
Subreach	Sample	D <sub>50</sub> (mm)	D <sub>84</sub> (mm)	Percent Sand (%)
1.1	Avg RR1,RR2	2.5	13.0	46
1.2	Avg RR1,RR2	2.5	13.0	46
1.3	Avg RR1,RR2	2.5	13.0	46
2.1	Avg RR1,RR2	2.5	13.0	46
2.2	Avg RR1,RR2	2.5	13.0	46
2.3	Avg RR1,RR2	2.5	13.0	46
2.4	Avg RR1,RR2	2.5	13.0	46
3.1	Avg WC1,RR3	12.6	28.5	20
3.2	Avg WC1,RR3	12.6	28.5	20
3.3	RR4	1.6	13.0	55
3.4	RR4	1.6	13.0	55
4	WC2*	25.3	72.4	15
5.1	Rep WPC	18.8	44.2	10
5.2	RR5	3.2	32.4	44
5.3	RR5	3.2	32.4	44
6.1	RR5	3.2	32.4	44
6.2	RR5	3.2	32.4	44
7	RR6	9.8	27.8	23
8.1	RR6	9.8	27.8	23
8.2	Wtd Avg RR6, RR7	9.5	24.7	24
8.3	Wtd Avg RR6, RR7	9.1	24.0	25
8.4	Wtd Avg RR6, RR7	8.5	23.2	26
9.1	Wtd Avg RR6, RR7	7.8	22.3	28
9.2	RR7	7.4	21.9	29
9.3	RR7	7.4	21.9	29
9.4	WC2*	25.3	72.4	15
10.1	RR7	7.4	21.9	29
10.2	RR4	1.6	13.0	55
<b>Tributaries</b>				
Hale Ck.	Hale-1	0.7	5.4	70
104th S.D.	104-1	3.3	14.5	41
Whitnall Park Ck.	Rep WPC	18.8	44.2	10
East Branch	EB-1	12.0	34.9	22

\*Adjusted to include 15 percent sand.

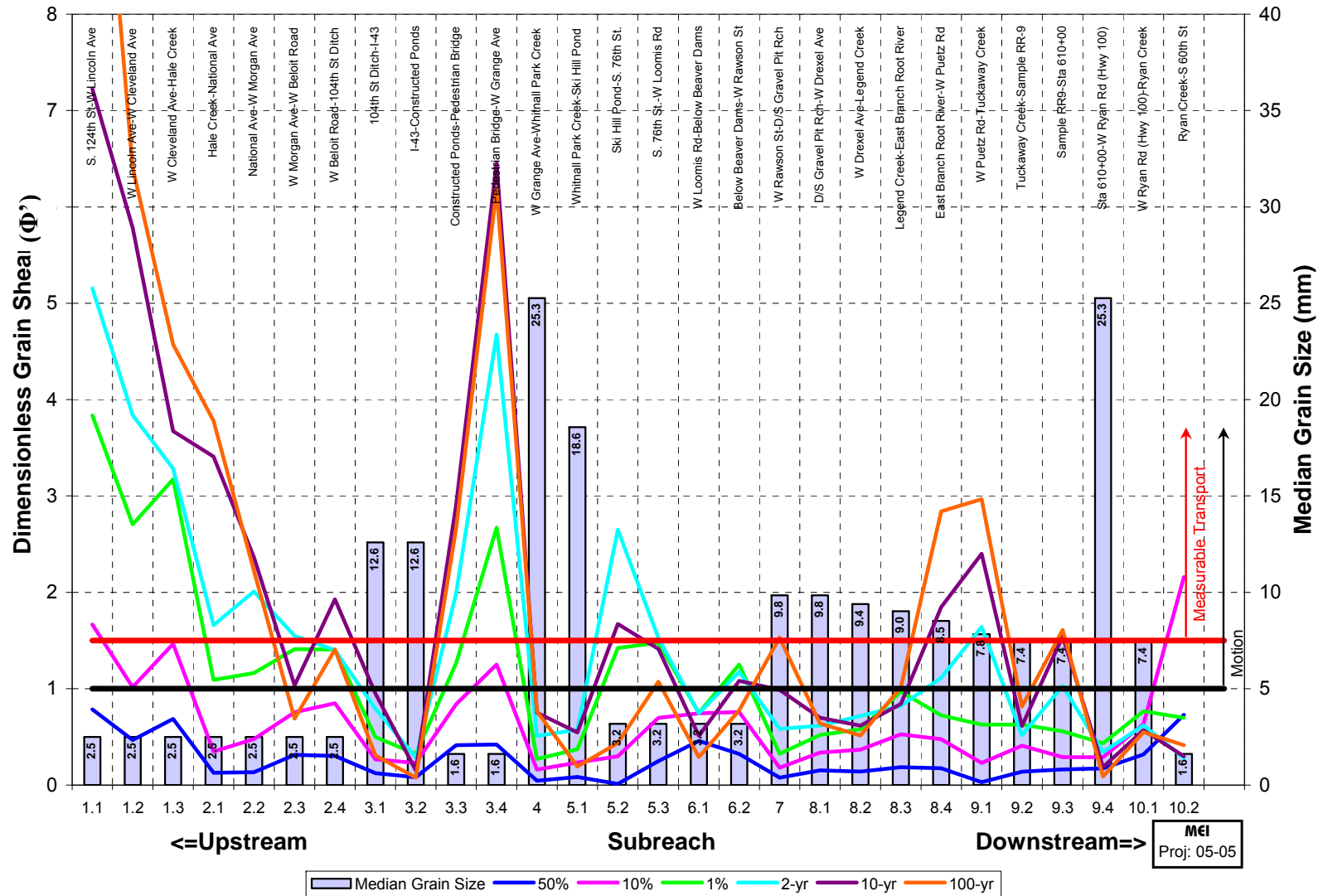


Figure 3.1. Results from the incipient motion analysis and the representative median grain size, by subreach. (A dimensionless grain shear value of 1.0 indicates incipient-motion conditions, and a value of 1.5 indicates measurable transport).

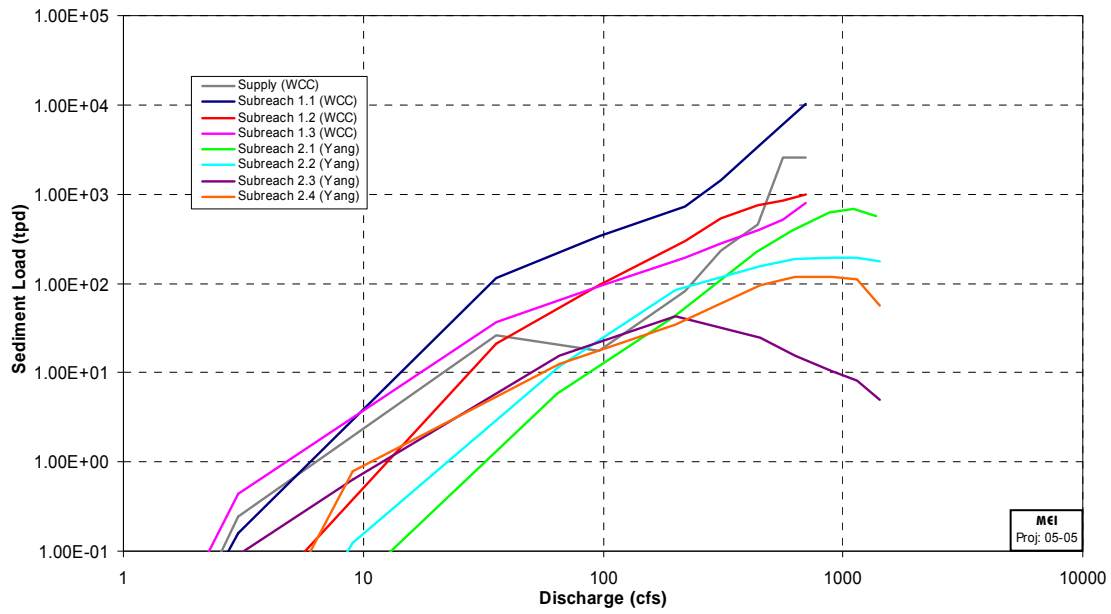


Figure 4.1a. Bed-material sediment-rating curves for the upstream supply and Subreaches 1.1 through 2.4.

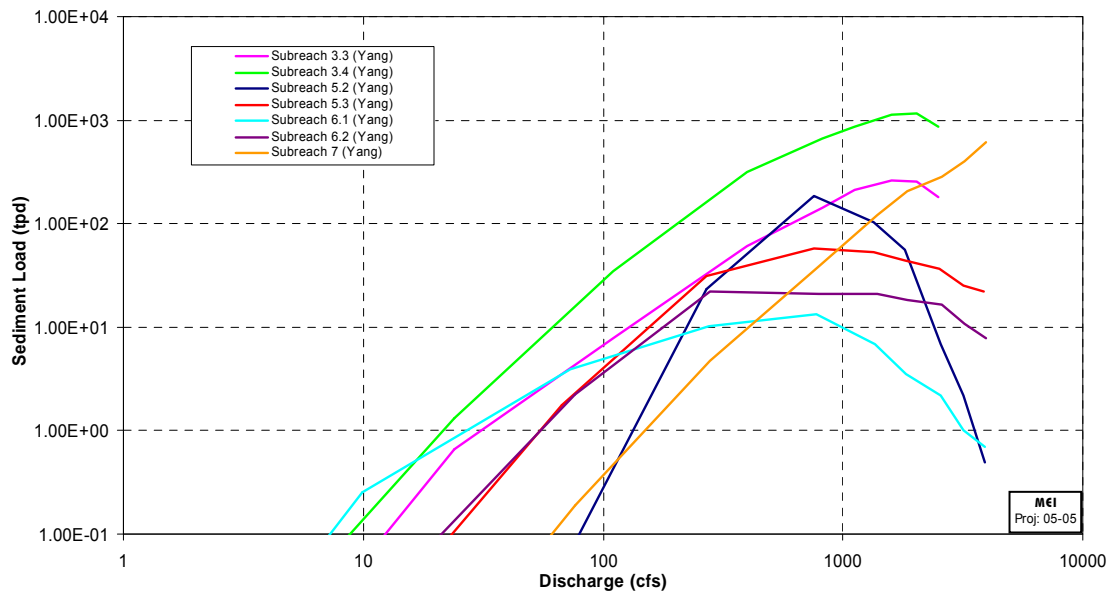


Figure 4.1b. Bed material sediment rating curves for the upstream supply and Subreaches 3.3 through 7.

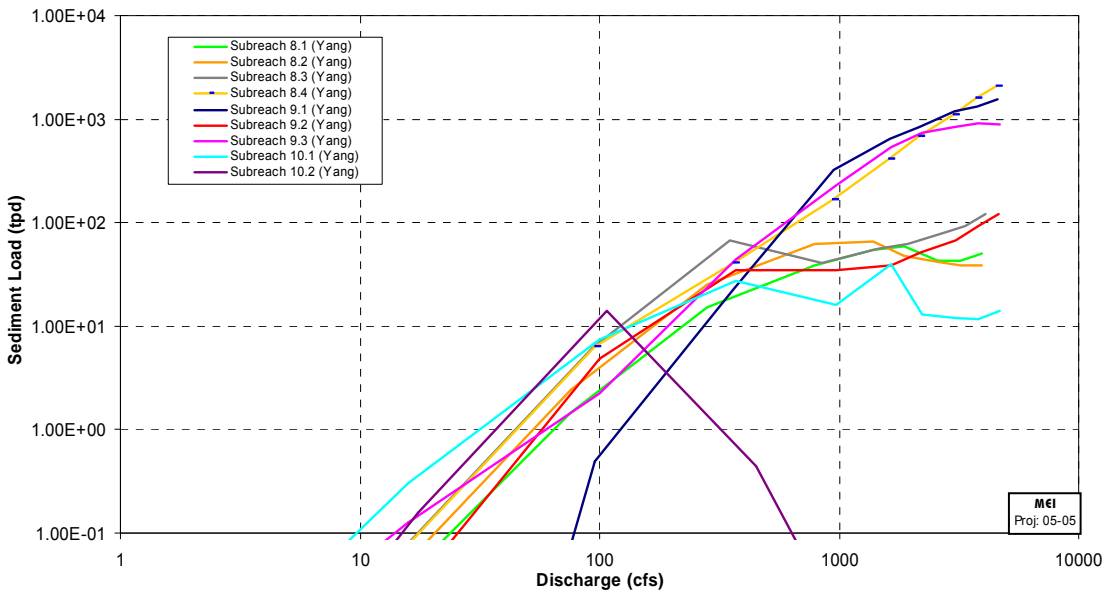


Figure 4.1c. Bed-material sediment-rating curves for the upstream supply and Subreaches 8.1 through 10.2.

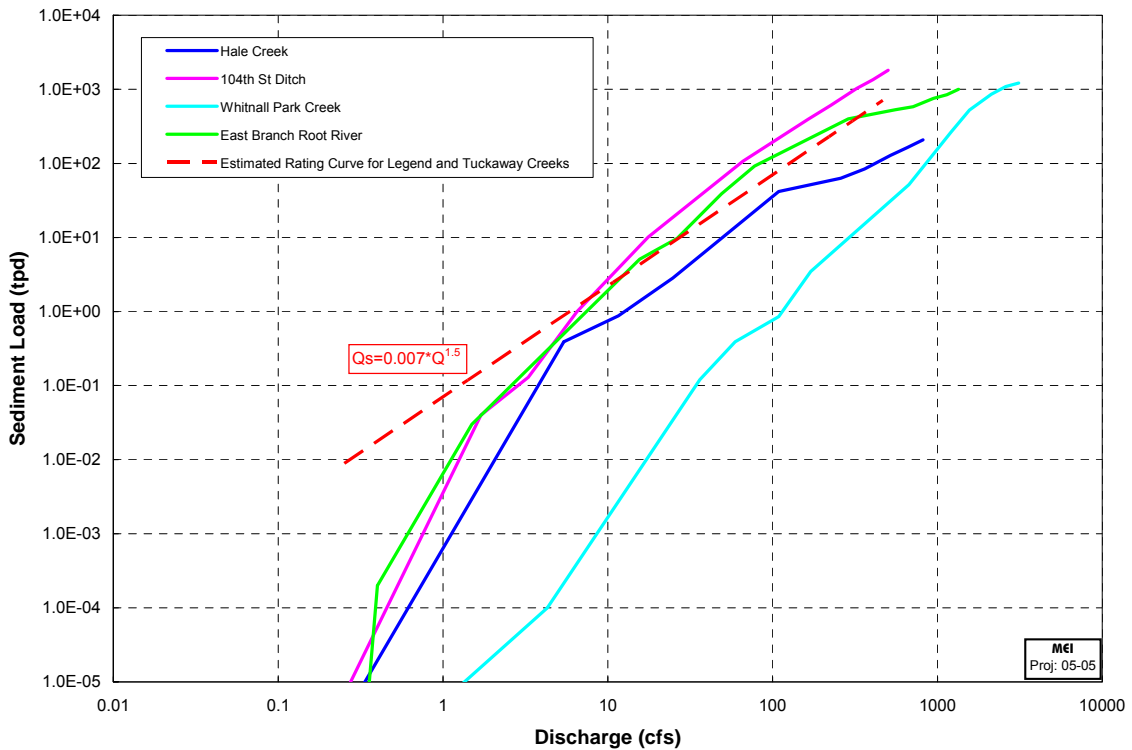


Figure 4.2. Bed-material sediment rating curves for the primary tributaries to the North Branch Root River.

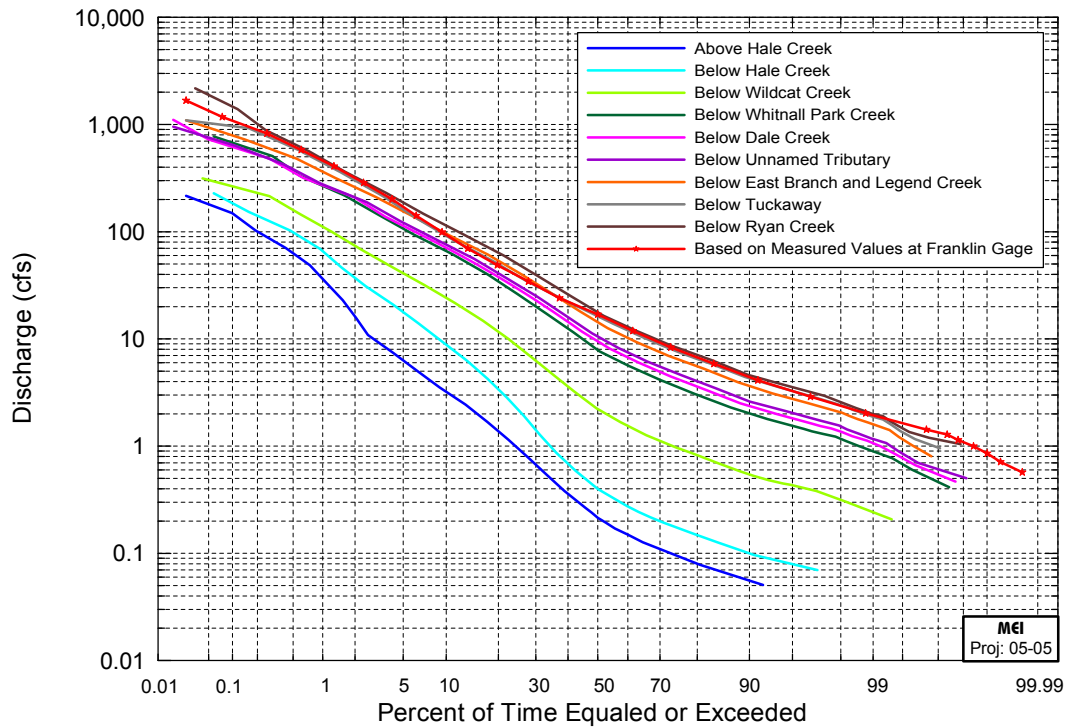


Figure 4.3. Existing conditions flow-duration curves at various locations along the North Branch Root River (see Technical Memorandum: Hydrology).

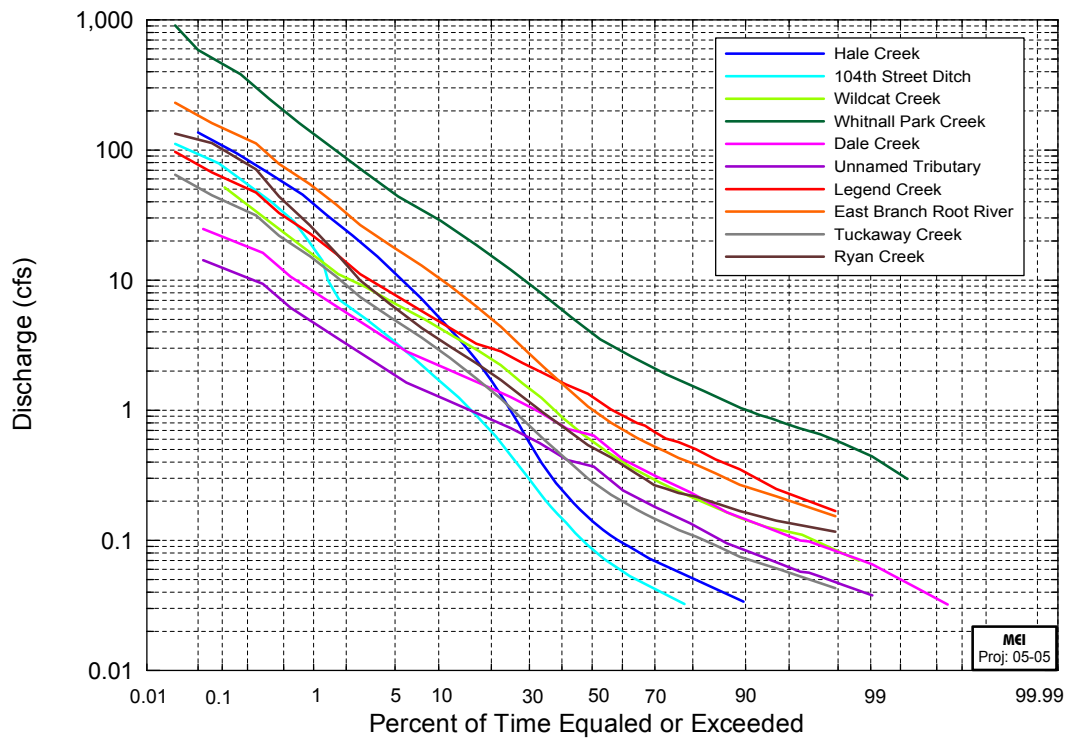


Figure 4.4. Existing conditions flow duration curves for the primary tributaries to the North Branch Root River (see Technical Memorandum: Hydrology).

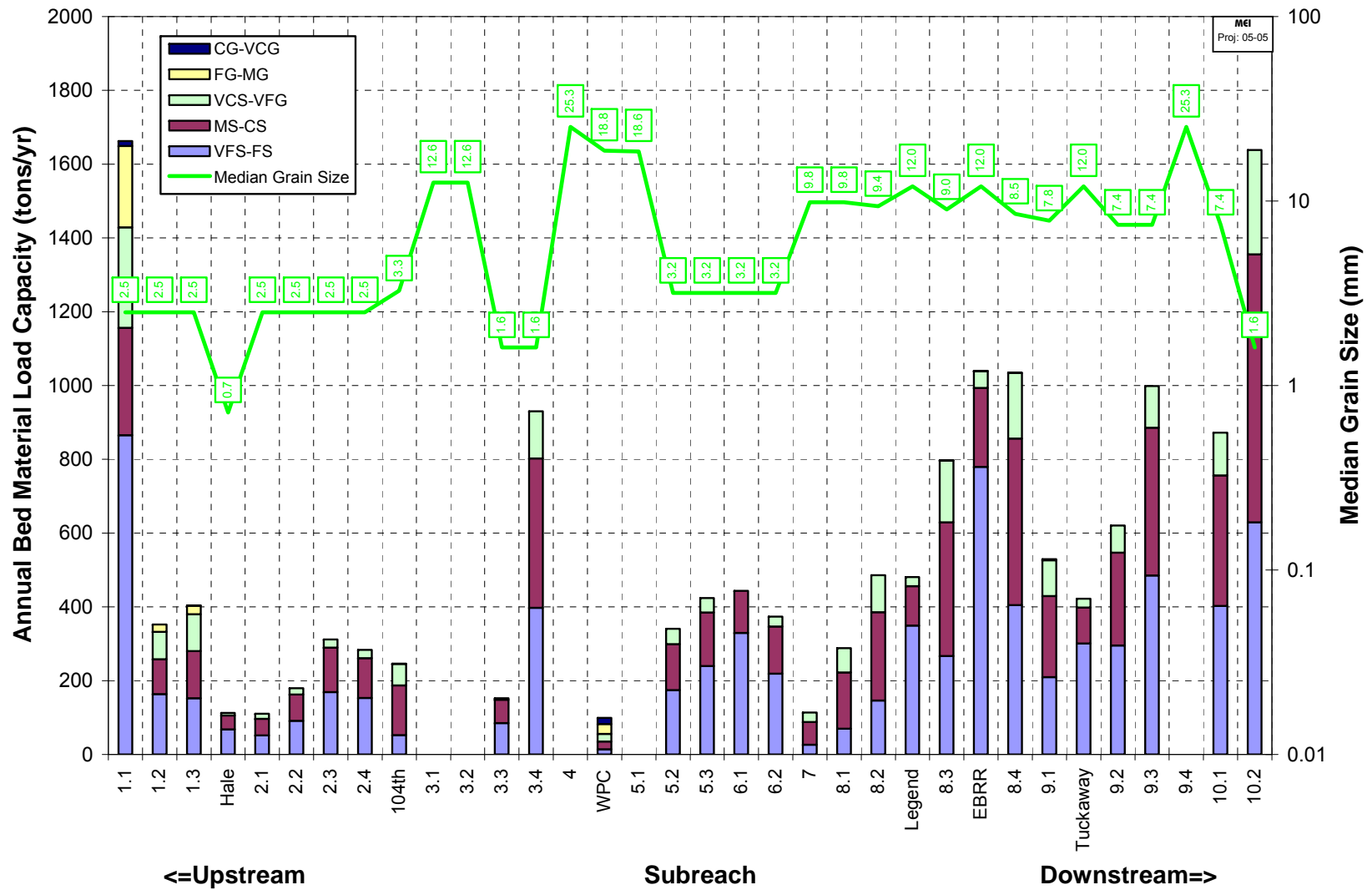


Figure 4.5. Average annual sediment transport capacity volumes (by size class) for the subreaches in the North Branch Root River and in the primary tributaries. Also shown is the median grain size of the bed material.

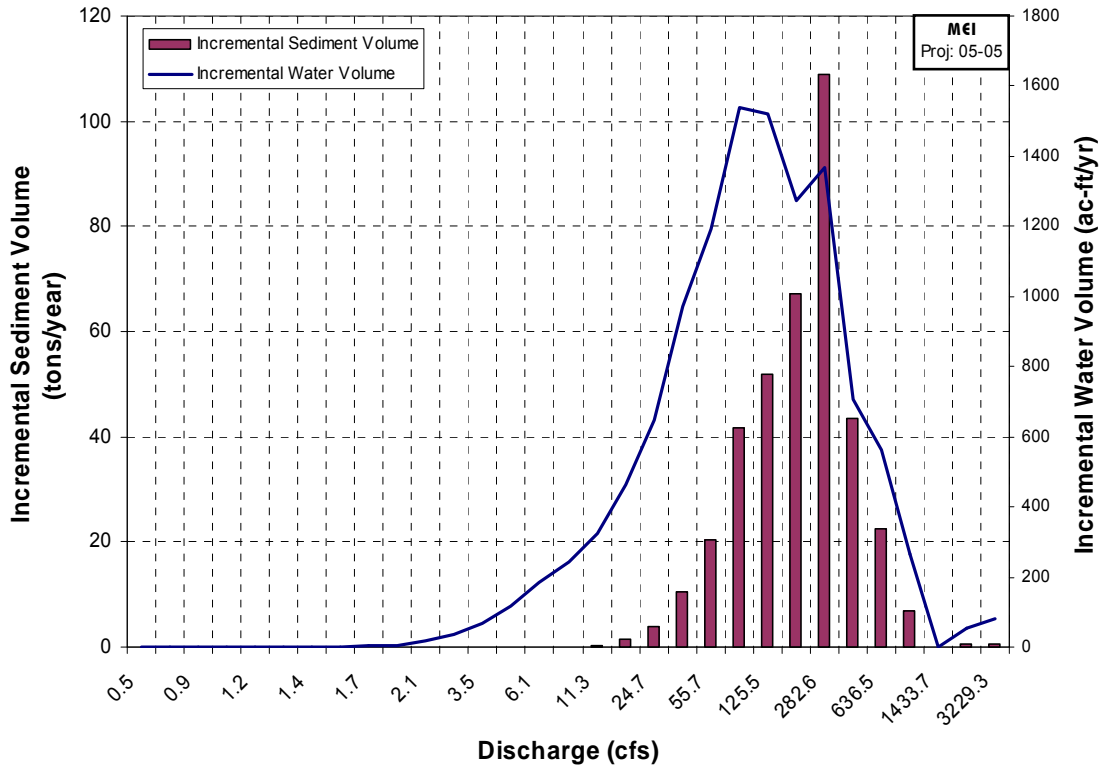


Figure 4.6. Example histogram of incremental bed-material load by discharge class for Subreach 6.2. Also shown is the incremental water volume within each discharge class.

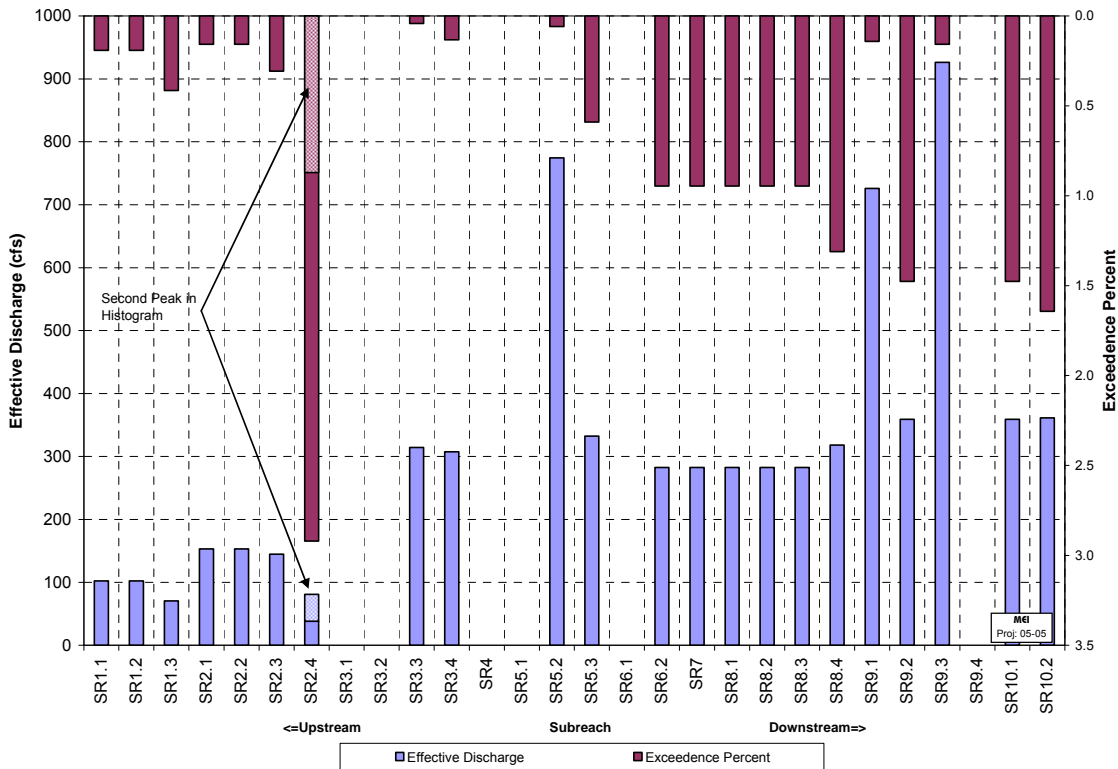


Figure 4.7. Results from the effective discharge analysis.

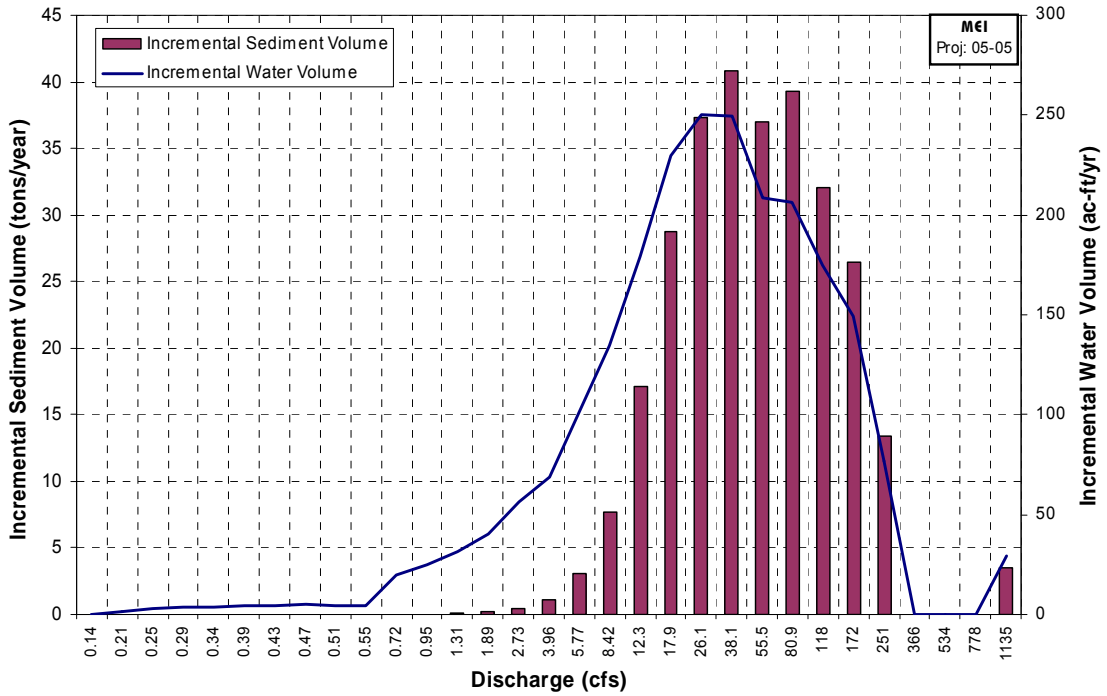


Figure 4.8. Histogram of incremental bed-material load by discharge class for Subreach 2.4. Also shown is the incremental water volume within each discharge class.

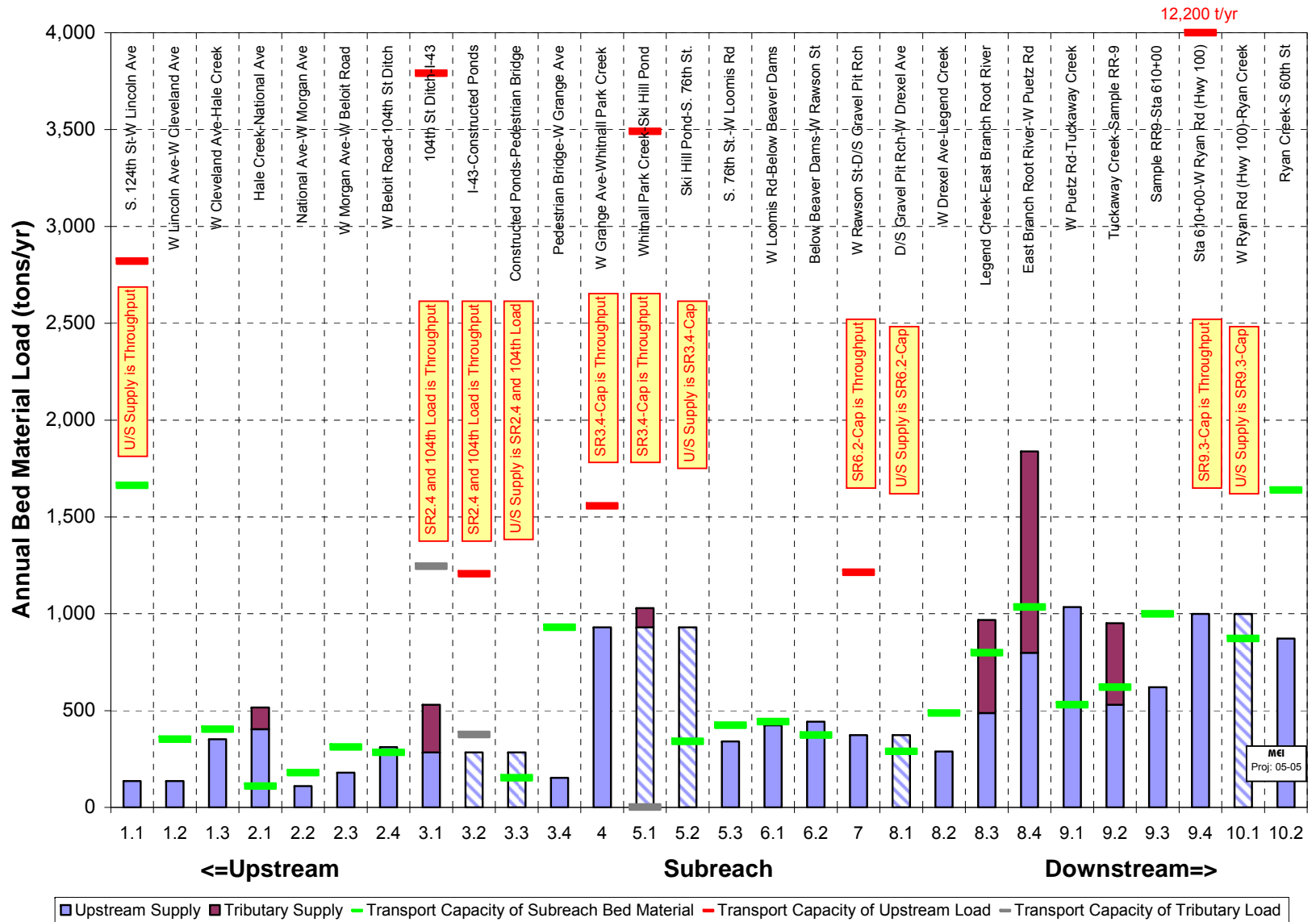


Figure 5.1. Comparison of annual bed material transport capacity and supply for each subreach.

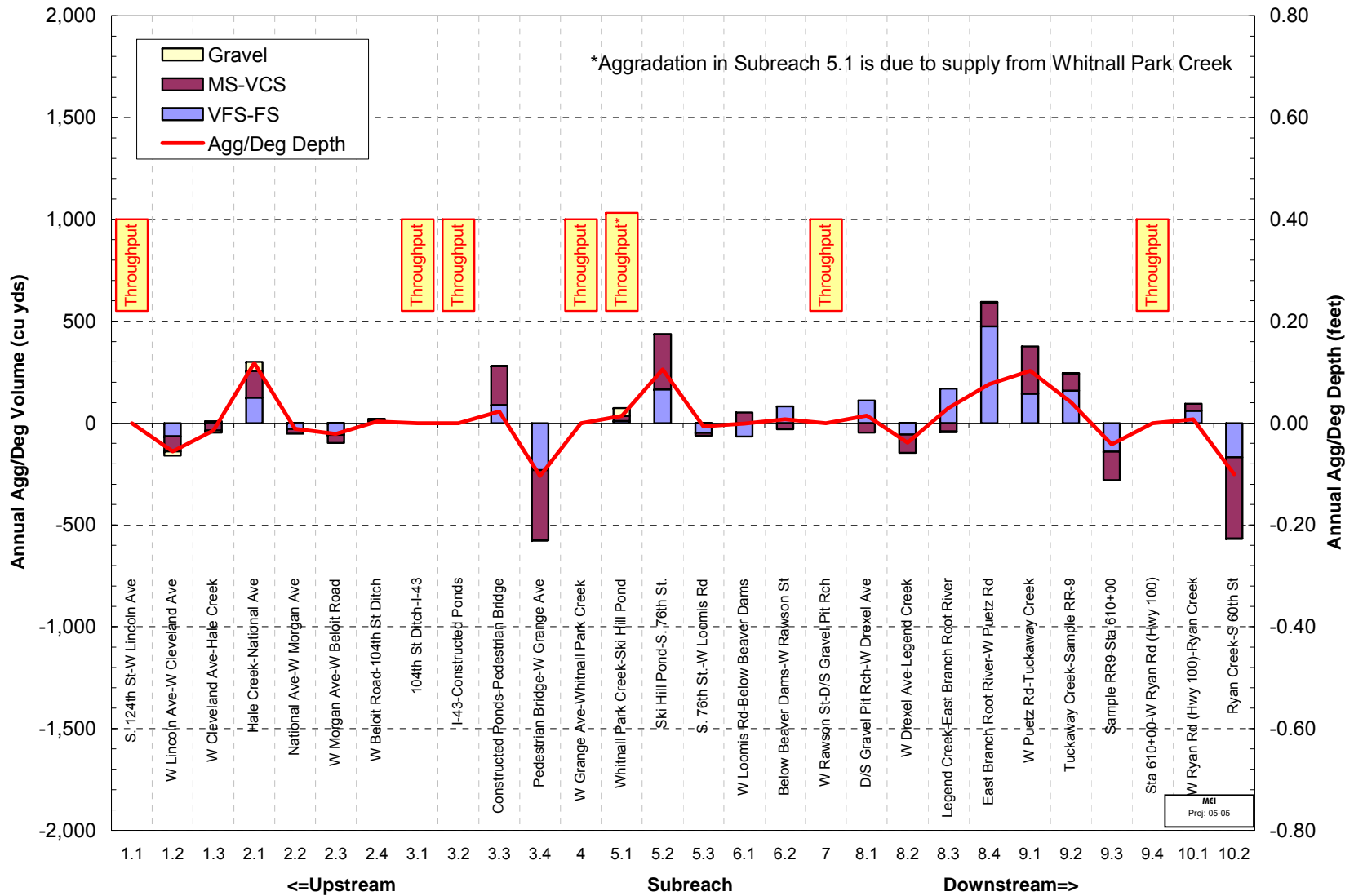


Figure 5.2. Computed volume of aggradation or degradation, by size fraction, in each of the subreaches from the sediment-continuity analysis. Also shown is the corresponding average depth of aggradation and degradation.

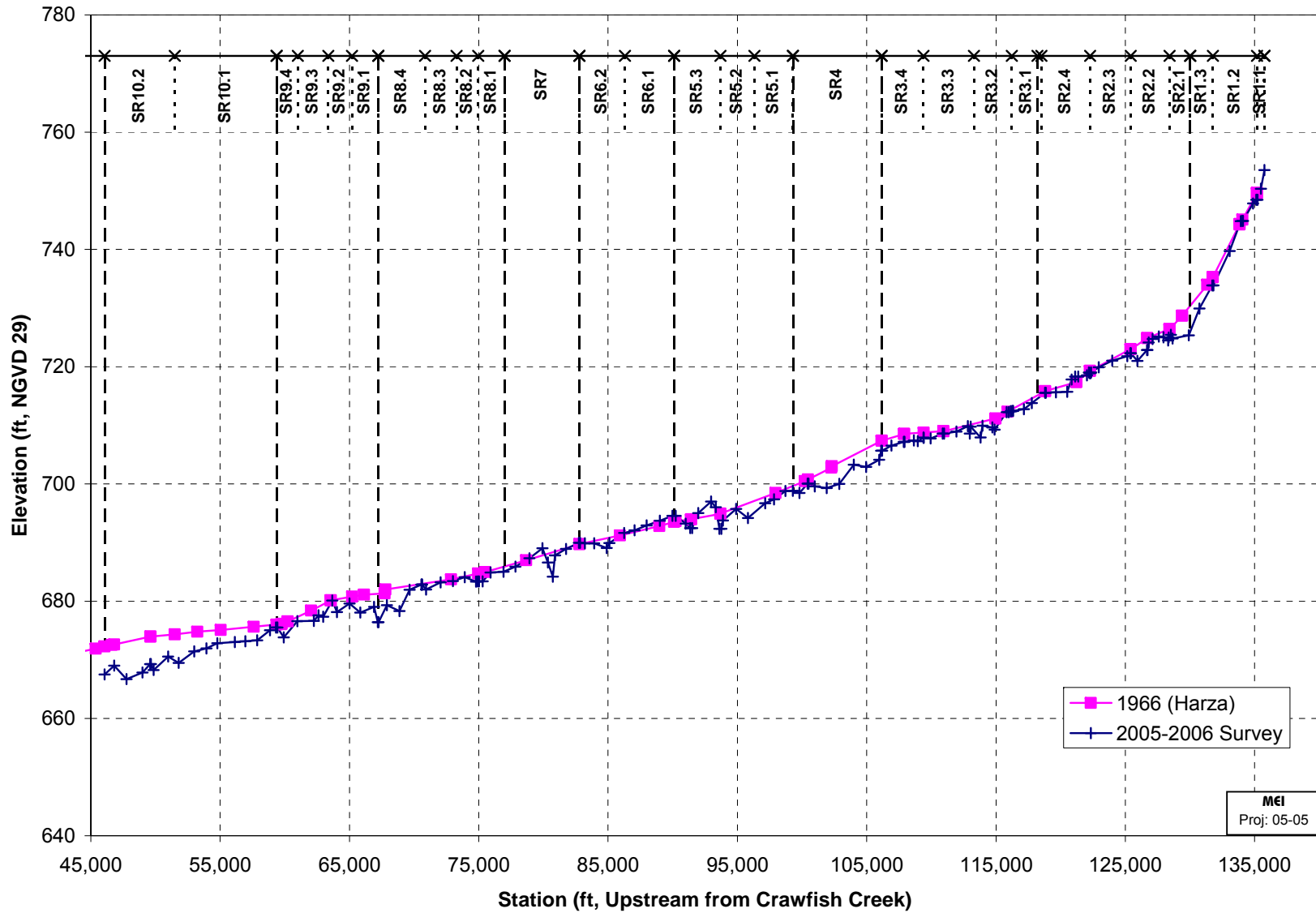


Figure 5.3. Comparative thalweg profiles for the North Branch Root River between 1966 and 2006.

Table 5.1. Summary of computed aggradation/degradation depths and observed trends of aggradation and degradation, by subreach.			
Subreach	Computed Change in Bed Elevation (ft)	MEI Observed Aggradation/Degradation Trends	Annual Change in Bed Elevation (1966 and 2006 Profiles, ft)
1.1	0.00	No agg/deg (bed protection)	NA*
1.2	-0.06	Moderately degradational	-0.02
1.3	-0.01	Moderately degradational	-0.05
2.1	0.12	Moderately aggradational	-0.08
2.2	-0.01	No observed agg/deg	-0.03
2.3	-0.02	No observed agg/deg	-0.01
2.4	0.00	No observed agg/deg	-0.01
3.1	0.00	No agg/deg (coarse bed matl)	NA*
3.2	0.00	No agg/deg (coarse bed matl)	-0.03
3.3	0.02	No observed agg/deg	-0.01
3.4	-0.10	Slightly degradational	-0.03
4	0.00	No agg/deg (gravel riffles, throughput)	-0.06
5.1	0.01	Slightly aggradational (due to WPC loads)	NA*
5.2	0.11	Moderately aggradational	NA*
5.3	-0.01	No observed agg/deg	0.01
6.1	0.00	No observed agg/deg	NA*
6.2	0.01	No observed agg/deg	-0.01
7	0.00	No agg/deg	-0.01
8.1	0.01	No observed agg/deg	-0.02
8.2	-0.04	Slightly degradational	NA*
8.3	0.03	No observed agg/deg	-0.01
8.4	0.08	Slightly aggradational	-0.05
9.1	0.10	Slightly aggradational	-0.07
9.2	0.04	Slightly aggradational	-0.03
9.3	-0.04	Slightly degradational	-0.04
9.4	0.00	No agg/deg (cobble bed, boulder step-pools)	-0.04
10.1	0.01	No observed agg/deg	-0.06
10.2	-0.03	Slightly degradational	-0.12

\*NA indicates insufficient resolution in 1966 profile to determine change in bed elevation.

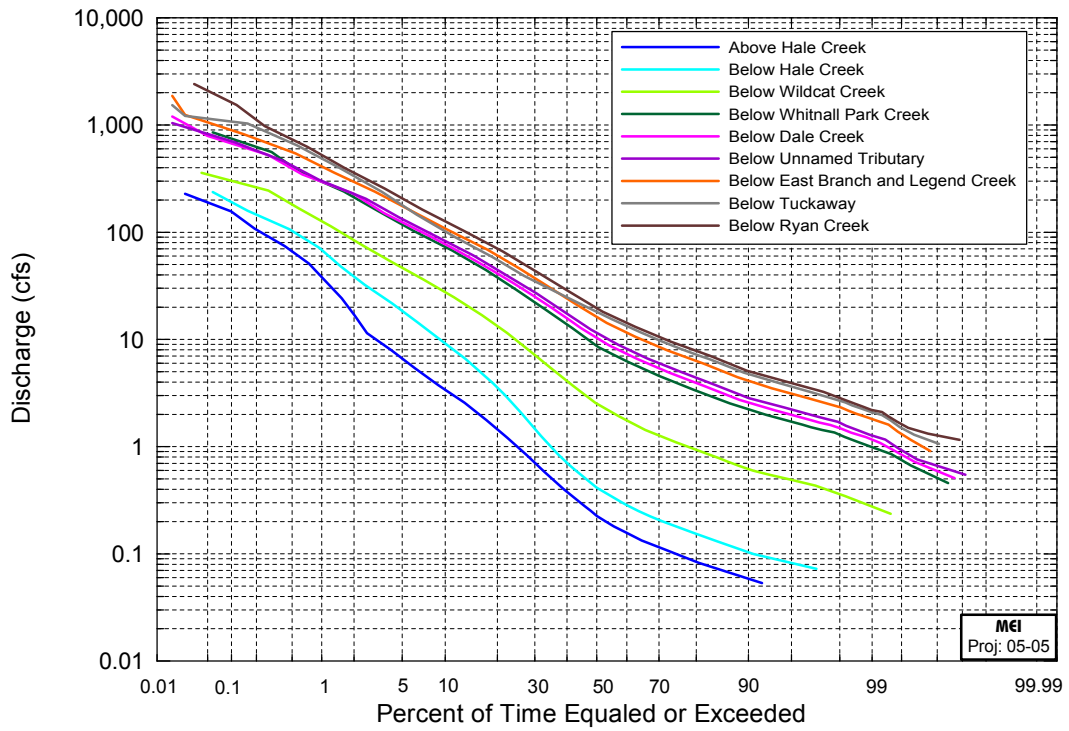


Figure 6.1. Future (2020) conditions flow-duration curves at various locations along the North Branch Root River (see Technical Memorandum: Hydrology).

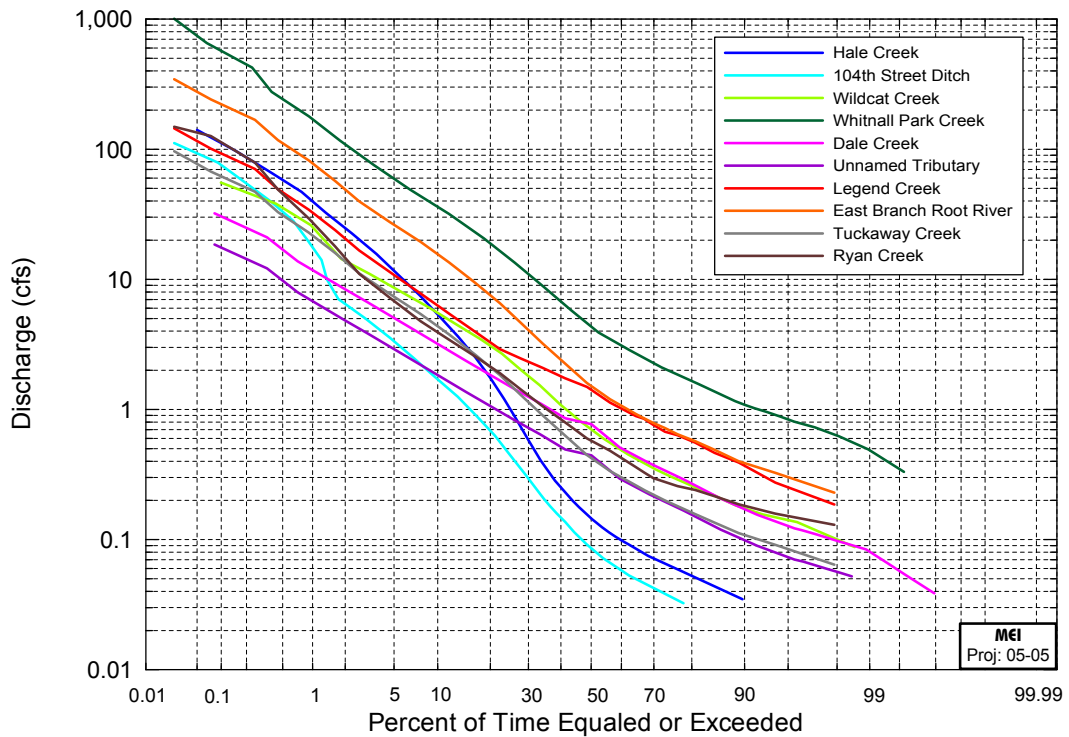


Figure 6.2. Future (2020) conditions flow duration curves for the primary tributaries to the North Branch Root River (see Technical Memorandum: Hydrology).

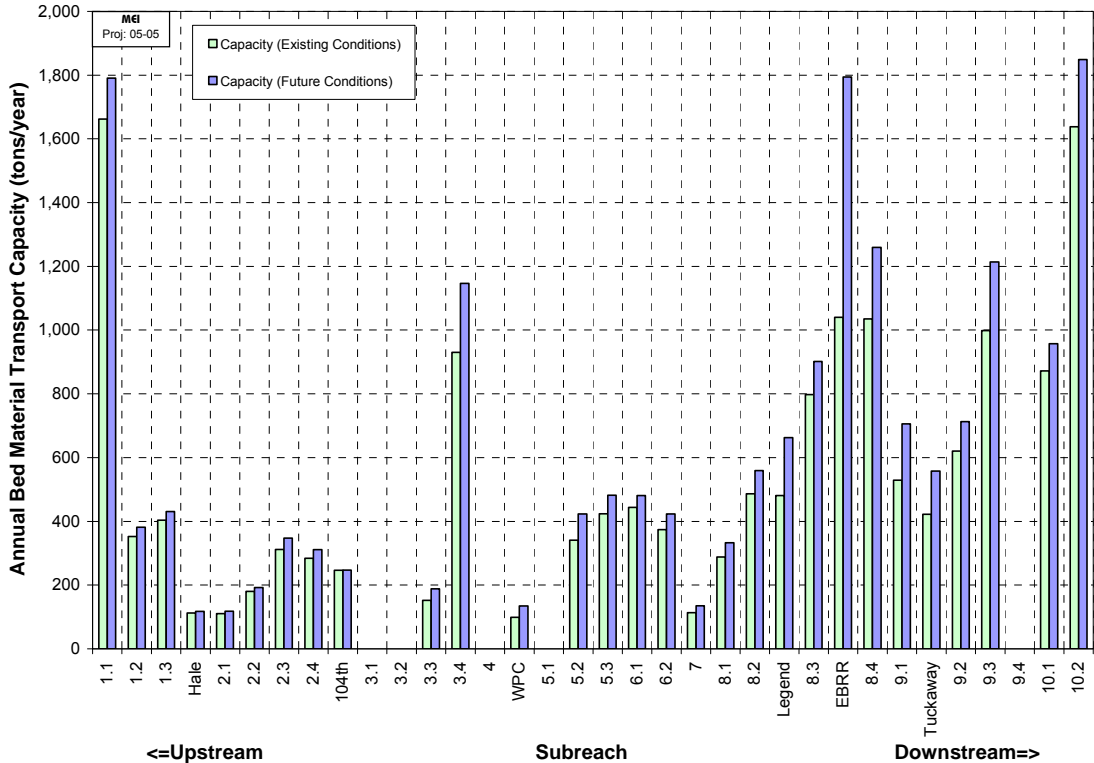


Figure 6.3. Annual bed-material transport capacity volumes under existing and future (2020) hydrologic conditions for the subreaches in the North Branch Root River and the primary tributaries.

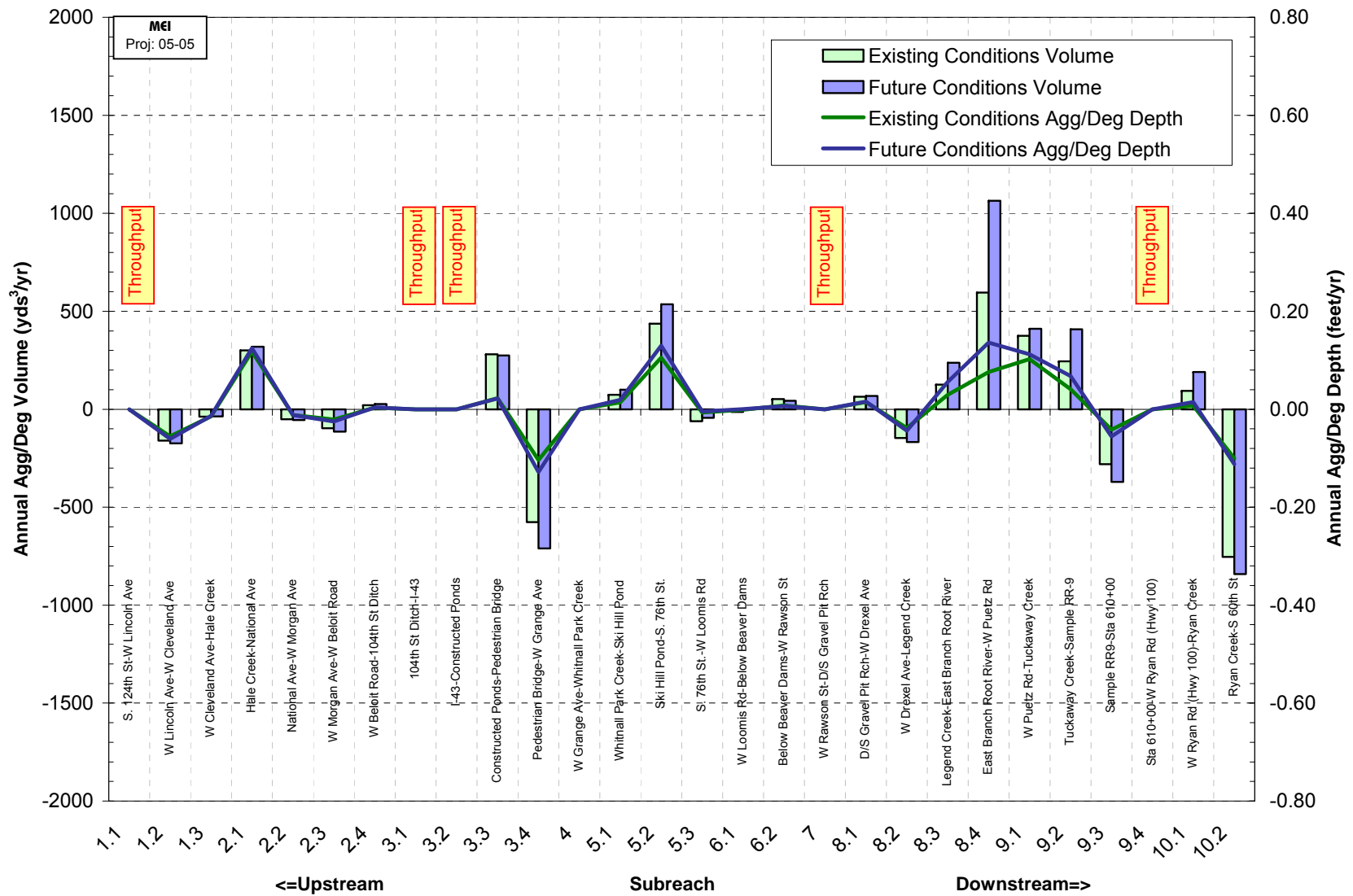


Figure 6.4. Computed annual volume of aggradation or degradation under existing and future (2020) hydrologic conditions for the subreaches in the North Branch Root River and the primary tributaries. Also shown is the corresponding change in bed elevation.